Published in final edited form as:

Nat Med. 2021 August ; 27(8): 1401–1409. doi:10.1038/s41591-021-01383-w.

Integrated genomic, epidemiologic investigation of *Candida auris* skin colonization in a skilled nursing facility

Diana M. Proctor[1], **Thelma Dangana**[2], **D. Joseph Sexton**[3], **Christine Fukuda**[2], **Rachel D. Yelin**[2], **Mary Stanley**[2], **Pamela B. Bell**[2], **Sangeetha Baskaran**[2], **Clay Deming**[1], **Qiong Chen**[1], **Sean Conlan**[1], **Morgan Park**[4],

NISC Comparative Sequencing Program[*],

Rory M. Welsh[3], **Snigdha Vallabhaneni**[3,5], **Tom Chiller**[3], **Kaitlin Forsberg**[3], **Stephanie R. Black**[6], **Massimo Pacilli**[6], **Heidi H. Kong**[7], **Michael Y. Lin**[2], **Michael E. Schoeny**[8], **Anastasia P. Litvintseva**[3], **Julia A. Segre**[1,9], **Mary K. Hayden**[2,9]

[1]Microbial Genomics Section, Translational and Functional Genomics Branch, National Human Genome Research Institute, National Institutes of Health, Bethesda, MD, USA.

[2]Department of Internal Medicine, Division of Infectious Diseases, Rush University Medical Center, Chicago, IL, USA.

[3]Mycotic Diseases Branch, Centers for Disease Control and Prevention, Atlanta, GA, USA.

[4]NIH Intramural Sequencing Center, National Human Genome Research Institute, National Institutes of Health, Bethesda, MD, USA.

[5]Division of Healthcare Quality Promotion, NCEZID, CDC, Atlanta, GA, USA.

Correspondence and requests for materials should be addressed to J.A.S. or M.K.H. jsegre@nhgri.nih.gov; mhayden@rush.edu.

[*]A list of authors and their affiliations appears at the end of the paper.

Author contributions

M.K.H., M.Y.L., A.P.L., S.V. and J.A.S. conceived the study. M.K.H., M.Y.L., A.P.L., S.V., J.A.S., T.C., K.F., S.R.B., M. Pacilli, T.D., M.E.S., and H.H.K. participated in clinical study design. T.D., C.F., R.D.Y., C.D., Q.C., S.C., M. Stanley, P.B.B., S. Baskaran, the NISC Comparative Sequencing Program, R.M.W., D.J.S. and D.M.P. collected and/or processed samples. D.M.P., M.E.S., C.F., R.D.Y. and M. Park performed analyses. D.M.P., M.K.H., M.E.S., M.Y.L. and J.A.S. wrote the manuscript. All authors read, edited and approved the manuscript.

NISC Comparative Sequencing Program

Jim Mullikin[4], Jim Thomas[4], Alice Young[4], Gerry Bouffard[4], Betty Barnabas[4], Shelise Brooks[4], Joel Han[4], Shi-ling Ho[4], Juyun Kim[4], Richelle Legaspi[4], Quino Maduro[4], Holly Marfani[4], Casandra Montemayor[4], Nancy Riebow[4], Karen Schandler[4], Brian Schmidt[4], Christina Sison[4], Mal Stantripop[4], Sean Black[4], Mila Dekhtyar[4], Cathy Masiello[4], Jenny McDowell[4], Morgan Park[4], Pam Thomas[4] and Meg Vemulapalli[4]

Competing interests

M.K.H. has been a co-investigator on several research studies for which Sage Products (now part of Stryker Corporation), Molnlycke and Medline provided chlorhexidine products at no charge to hospitals and skilled nursing facilities participating in the research. Neither M.K.H. nor her employer (Rush University Medical Center) received chlorhexidine products. M.Y.L. has received research support in the form of contributed product from Sage Products (now part of Stryker Corporation) and has received an investigator-initiated grant from the CareFusion Foundation (now part of BD). All other authors declare no competing interests.

Additional information

Extended data is available for this paper at https://doi.org/10.1038/s41591-021-01383-w.

Supplementary information The online version contains supplementary material available at https://doi.org/10.1038/s41591-021-01383-w.

Peer review information *Nature Medicine* thanks Tobias Hohl, Sudha Chaturvedi and Iliyan Iliev for their contribution to the peer review of this work. Alison Farrell was the primary editor on this article and managed its editorial process and peer review in collaboration with the rest of the editorial team.

[6]Communicable Disease Program, Chicago Department of Public Health, Chicago, IL, USA.

[7]Dermatology Branch, National Institute of Arthritis and Musculoskeletal and Skin Diseases, National Institutes of Health, Bethesda, MD, USA.

[8]College of Nursing, Rush University, Chicago, IL, USA.

[9]These authors contributed equally: Julia A. Segre, Mary K. Hayden.

Abstract

Candida auris is a fungal pathogen of high concern due to its ability to cause healthcare-associated infections and outbreaks, its resistance to antimicrobials and disinfectants and its persistence on human skin and in the inanimate environment. To inform surveillance and future mitigation strategies, we defined the extent of skin colonization and explored the microbiome associated with *C. auris* colonization. We collected swab specimens and clinical data at three times points between January and April 2019 from 57 residents (up to ten body sites each) of a ventilator-capable skilled nursing facility with endemic *C. auris* and routine chlorhexidine gluconate (CHG) bathing. Integrating microbial-genomic and epidemiologic data revealed occult *C. auris* colonization of multiple body sites not targeted commonly for screening. High concentrations of CHG were associated with suppression of *C. auris* growth but not with deleterious perturbation of commensal microbes. Modeling human mycobiome dynamics provided insight into underlying alterations to the skin fungal community as a possible modifiable risk factor for acquisition and persistence of *C. auris*. Failure to detect the extensive, disparate niches of *C. auris* colonization may reduce the effectiveness of infection-prevention measures that target colonized residents, highlighting the importance of universal strate- gies to reduce *C. auris* transmission.

C. auris has emerged as a human pathogen of high concern due to its extensive antifungal resistance, high mortality rates associated with invasive infections and its potential to cause healthcare-associated outbreaks[1–3]. A recent systematic review of nearly 5,000 cases of *C. auris* from 33 countries reported an overall crude mortality rate of 39%[4]. The US Centers for Disease Control and Prevention (CDC) have declared *C. auris* to be an urgent public health threat, the first fungal pathogen to receive this designation[5]. Persistent skin colonization[6] likely contributes to the epidemic potential of *C. auris*. Healthcare providers may contaminate their hands, gloves or clothing with *C. auris* by touching the skin of a colonized patient. *C. auris* can then be transmitted to another patient if the healthcare provider fails to perform adequate hand hygiene or adhere to other infection-prevention measures. Additionally, shedding from colonized patients' skin into the healthcare environment, calculated to occur at a rate of a million microbes per hour[7], creates an environmental reservoir and source of ongoing nosocomial transmission[8–11]. In the US, high-acuity long-term care facilities such as long-term acute care hospitals and ventilator-capable skilled nursing facilities have reported high prevalence of *C. auris*, and there is concern that these facilities may serve as drivers of regional *C. auris* spread[2,3,12,13].

Effective infection-control measures play a central role in the management of *C. auris* because frequent resistance to multiple classes of antifungal agents (that is, azoles, polyenes, echinocandins) limits treatment options for invasive infection[14–16]. Constraining

effective infection control is the paucity of published data concerning the spatial extent of skin colonization by *C. auris* and clarity on the relative sensitivity of different body sites to identify residents colonized with *C. auris*. Occult colonization has been shown to underlie transmission in recalcitrant outbreaks involving other pathogens, including *Klebsiella pneumoniae*[17]. Efficacy of the bis-biguanide antiseptic CHG in controlling *C. auris* colonization is another uncertainty. While CHG bathing is a common component of multimodal *C. auris* control programs in acute and long-term care settings, previous investigators have reported persistent colonization of residents, environmental contamination and ongoing *C. auris* transmission despite CHG bathing[9,12,18].

C. auris was first detected in metropolitan Chicago, IL, in 2016, where post-acute care facilities have become epicenters for this pathogen[3,12]. Here we report on an integrated clinical research program to study *C. auris* colonization of residents at a ventilator-capable skilled nursing facility in Chicago with endemic *C. auris* and routine CHG bathing. We conducted serial point prevalence surveys of skin, oral and perianal sites to investigate *C. auris* using culture-dependent and culture-independent methods and analyzed the relationship of CHG concentration with growth of *C. auris* and the skin microbiota. Phylogenetic marker genes of bacterial and fungal communities (16S rRNA and internal transcribed spacer (ITS)1, respectively) permit high-resolution investigation into the microbiome associated with clinical samples. To understand community dynamics of *C. auris* skin colonization, we investigated the temporal stability and diversity of skin, oral and gut bacterial and fungal communities.

Results

Overview of study participants.

We conducted three monthly point prevalence surveys between January and April 2019 on the ventilator ward of a skilled nursing facility in Chicago, IL. At the time of each survey, research personnel collected swab specimens from up to ten body sites (anterior nares, external auditory canal, axilla, inguinal crease, perianal skin, toe web, palm and fingertips, buccal mucosa and tongue and tracheostomy site) for semiquantitative (n = 1,358) and quantitative (n = 424) *C. auris* culture, microbiome analysis (n = 1,358) and quantification of CHG concentration (n = 813) (Supplementary Table 1). Clinical data were collected at bedside from electronic medical records and recorded onto standardized data-collection forms. Fifty-seven (72%) of 79 unique residents on the ward during the study period participated, and, of those participating, 49 (86%) residents were found to be colonized with *C. auris* at one or more body site in one or more survey. Overall, residents were older adults, had a history of colonization or infection with carbapenem-resistant bacteria and had long lengths of stay before the first date of sample collection (Table 1). Residents with *C. auris* colonization were more likely to require an invasive medical device (for example, gastrostomy tube, mechanical ventilation) and were more likely to have received antibacterial agents in the 90 d before the first sample collection. While no participant developed *C. auris* clinical infection during the study period, review of clinical microbiology data from the time of admission through 6 months after the last survey identified one

resident with *a C. auris* bloodstream infection 6 weeks before sample collection and two residents with *C. auris* bloodstream infections in the 6 months after the surveys concluded.

All isolates were susceptible to the commonly used antifungal agents fluconazole, amphotericin B and micafungin (Supplementary Table 2). Genomes and ITS1 sequences of *C. auris* isolates matched those of the South American clade IV[19]. Between isolates, the number of single-nucleotide variants ranged from one to 20 (mean = 14, $N = 4$) when reads were mapped to a nanopore reference genome generated from an isolate from this outbreak, consistent with clonality within the facility.

Patterns of body-site colonization with *C. auris*.

To identify the spatial extent of *C. auris* colonization across the human body, we surveyed ten body sites with both culturing and microbial sequencing (Extended Data Fig. 1). Patterns of body-site colonization were highly individualized (Extended Data Fig. 2). Across all study participants, the frequency of colonization varied by body site: 42.9% of residents tested positive at nares, 40.4% of residents tested positive at palms and/or fingertips, and 35.7% of residents tested positive at toe webs (Fig. 1a). Importantly, residents who were culture negative at commonly targeted screening sites (here only unilaterally sampled axilla, inguinal crease and/or nares) were frequently colonized at other body sites, such as palms and/or fingertips. Of those who were colonized, 30.4% were colonized at a single body site, with monocolonization most commonly occurring at either the anterior nares or palms and/or fingertips (Extended Data Fig. 2). *C. auris* never monocolonized the buccal mucosa, tongue, neck, tracheostomy site or external auditory canal.

Because most colonized residents (69.6%) were colonized at two or more sites, we next performed a sensitivity analysis to determine the combination of screening sites most effective at detecting the largest number of *C. auris*–colonized residents (Fig. 1b). Nares were the most sensitive single site, achieving 53.1% sensitivity. The most sensitive two-site combination was nares with palm and fingertips, with 76.1% sensitivity; adding toe webs increased sensitivity to 89.1%, and adding the perianal site and the inguinal crease increased sensitivity to 97.8%. Identification of all colonized residents was achieved by screening a minimum of six body sites (nares, palm and fingertips, toe webs, perianal skin, inguinal crease, axilla), consistent with the wide degree of variation observed in site-specific colonization with *C. auris*. The current recommended screening scheme collects a composite swab of a resident's bilateral axillae and inguinal creases[20], sometimes with the addition of anterior nares[21]. In our study, which was performed with unilateral sampling, these two- and three-site combinations achieved sensitivities of 61.9% and 79.7%, respectively.

As fungal load may contribute to a resident's risk of subsequent infection or of acting as a source of transmission through contaminating the environment or a healthcare provider, we quantified the bioburden of sites screened. The most densely colonized site was the nares, which exhibited a bimodal distribution with a median peak abundance of $10^{8.2}$ colony-forming units (CFU) (Extended Data Fig. 3). The axilla and inguinal crease harbored relatively low population densities: the axilla exhibited a uniform distribution with a median abundance of $10^{3.9}$ CFU, while the inguinal crease exhibited a bimodal distribution with two comparable peaks and a median abundance of $10^{4.9}$ CFU. Due to the semiquantitative nature

of plate culture counts, quantitative analyses were performed. The median most probable number (MPN) of *C. auris* in nares was significantly higher than that in the axilla or inguinal crease, and nares had the greatest proportion of samples with a high bioburden (Fig. 1c and Extended Data Fig. 4). Collectively, these data suggest that multifocal colonization occurs commonly and that sites other than those screened most commonly may harbor high population densities, which may contribute to recalcitrant outbreaks experienced by some facilities.

Effectiveness of CHG against *C. auris* colonization.

The skin antiseptic CHG is used routinely for bathing hospital residents to reduce multidrug-resistant-organism colonization and infection. Reports on the efficacy of CHG against colonization with *C. auris* have had mixed results[9,22,23]. As all residents of the ventilator-capable skilled nursing facility in the current study were undergoing routine bathing with 2% CHG-impregnated cloths, we sought to investigate the relation between CHG concentration on skin and growth of *C auris* in culture. Consistent with prior studies[24], we found that CHG concentrations varied by body site ($F(5,740) = 25.99$, $P < 0.001$; Fig. 2a). The highest concentrations of CHG were measured at the inguinal crease (median and IQR, 78.1 and 39.1–312.5 μg ml^{-1}), while relatively low concentrations were measured at the palm and/ or fingertips (median and IQR, 9.8 and 0–39.1 μg ml^{-1}) and the toe web (median and IQR, 4.9 and 0–19.5 μg ml^{-1}). As we observed that sites with the lowest CHG concentrations (palm and/or finger- tips, toe web) were colonized by *C. auris* at the highest frequencies (Fig. 1), we tested for an explicit association. We found evidence of a modest but not significant linear association between CHG concentration (log_2 transformed) and the odds of *C. auris* detection (odds ratio, 0.93; 95% confidence interval, 0.85–1.01; $P = .068$). Cut-point analysis revealed a significant reduction in the odds of *C. auris* colonization for CHG concentrations ≥625 μg ml^{-1} (odds ratio, 0.27; 95% confidence interval, 0.12–0.65; $P = 0.003$) (Fig. 2b). Importantly, the concentration of CHG needed to reduce the odds of colonization (≥625 μg ml^{-1}) was detected at only 7.3% of skin sites tested. Because data on the time of the most recent bath before CHG measurement were not available, we could not control for this variable. Nonetheless, we note that the concentration of 625 μg ml^{-1}, associated with reduced odds of *C. auris* colonization in situ, was 20–39 times higher than the minimum concentration of CHG required to inhibit the growth of *C. auris* in vitro (16–32 μg ml^{-1}) (Supplementary Table 2).

Underlying microbiome associated with *C. auris* colonization.

As *C. auris* must invade the microbiome to colonize human skin, we next explored associations between *C. auris* and features of the human microbiome. We characterized bacterial and fungal community composition by sequencing 16S rRNA and ITS1 regions from clinical samples collected during the first survey at each of ten body sites of 51 residents. While foundational studies of young healthy volunteers demonstrated *Malassezia* predominance of the skin mycobiome[25], the mycobiome of these skilled nursing facility residents was composed of multiple *Malassezia* and *Candida* species (Fig. 3a). *Candida* species found on the skin included a diverse constellation of *C. auris*, *Candida tropicalis*, *Candida parapsilosis*, *Candida albicans*, *Candida orthopsilosis*, *Candida duobushaemulonii*, *Candida glabrata*, *Candida krusei*, *Candida dubliniensis* and *Candida metapsilosis*, among

others. Sites exhibiting potential for *Candida* predominance included perianal skin, the axilla, nares, the inguinal crease, palms and/or fingertips and toe webs, overlapping with sites identified as commonly colonized with *C. auris* by culturing. More extensive comparisons between culture and sequence results highlighted confounding underlying biological principles. For example, while culturing may demonstrate a higher *C. auris* level in the nares than in the inguinal crease (Fig. 1c), sequencing results may not identify *C. auris* as the predominant species due to the diversity, composition and bioburden of the nares microbiome (Fig. 3a).

Next, we sought to identify bacterial species enriched in *C. auris*–colonized samples. In a sparse, partial-least-squares discriminant analysis (sPLS-DA), Proteobacteria *Proteus mirabilis*, *K. pneumoniae*, *Providencia stuartii* and *Pseudomonas aeruginosa* contributed most to segregation of *C. auris* culture-positive samples away from *C. auris* culture-negative samples (Fig. 3b–d). Conversely, the skin commensal *Staphylococcus hominis* primarily contributed to the segregation of culture-negative samples away from culture-positive samples. Other commensal species, including *Corynebacterium tuberculostearicum*, *Staphylococcus epidermidis*, *Staphylococcus caprae* and *Corynebacterium striatum*, were also found to have principal-component loading scores associated with *C. auris* culture negativity. Notably, *P. mirabilis* and *P. stuartii* were among a small set of taxa that exhibited a direct correlation with CHG concentration, indicating an association between increasing relative abundance of these species and increasing CHG concentrations (Extended Data Fig. 5).

Longitudinal analysis of *C. auris* colonization.

This longitudinal, observational clinical study was designed to explore microbiome alterations associated with *C. auris* acquisition and persistence. To explore mycobiome dynamics, the fungal community of samples from the monthly surveys was visualized by principal-coordinate analysis of the weighted UniFrac distance metric, which takes into account both phylogeny and relative abundance of taxa. Cluster analysis revealed four clusters or fungal community state types (CSTs) in the data (Extended Data Fig. 6). Predominance of either *Malassezia* (CST1, CST3) or *Candida* species (CST2, CST4) drove segregation of samples along the first major axis, which explained 61.3% of the variation (Fig. 4a). While genus-level differences defined axis 1, species-level variation drove segregation of communities along axis 2, which accounted for 14.6% of the variation.

CST1 best approximates a typical healthy skin commensal community[25], composed predominantly of *Malassezia restricta* and including other commensal *Malassezia* species: *Malassezia globosa*, *Malassezia furfur* and *Malassezia arunalokei* (Fig. 4b). CST2 was diverse with inclusion of multiple *Candida* spp., including *C. auris*, *C. albicans*, *C. tropicalis*, *C. parapsilosis*, *Candida orthopsilosis* and *C. metapsilosis*. The remaining CSTs were less diverse. CST3 was predominated by *Malassezia slooffiae*, with frequent high-abundance co-colonization by either *C. auris* or *M. restricta*. Most samples in CST4 were mono-predominated by *C. auris*, although a few samples were co-predominated by *M. restricta* or *C. parapsilosis*.

Next, we investigated mycobiome dynamics, using data from the first two surveys to model the probability that an individual body site would transition between CSTs (Fig. 4c). *Malassezia*-diverse CST1 was the most stable state with the highest self-transition ('remain the same') probability ($P = 0.82$). By contrast, CST2, with diverse *Candida* species, not typically abundant on healthy human skin, comprised the least stable community. CST2 samples were as likely to transition to CST4 (predominated by *C. auris*) as they were to remain as CST2 ($P = 0.38$). By contrast, *Malassezia*-diverse CST1 samples rarely transitioned toward *C. auris*–predominant CST4 ($P = 0.02$), with higher transition frequency toward the diverse *Candida* CST2 ($P = 0.07$) or *M. slooffiae*-dominated CST3 ($P = 0.09$). While *M. slooffiae*, *C. tropicalis* and *C. parapsilosis*[25–27] rarely dominate the skin microbiome of healthy volunteers, they are often found at low abundance and low prevalence in skin communities. In sum, these data suggest potential value in monitoring or intervening at the intermediate state when the skin community migrates away from the diverse commensal *Malassezia* community.

To gain further insight into the stability of *C. auris* colonization, we used a Markov chain built from the first two point prevlence surveys to predict the number of samples in each CST at the third-point prevalence survey and to forecast patterns at time points beyond the study interval. This model predicts *C. auris*–colonization prevalence at the third-point prevalence survey (Fig. 4d) and forecasts persistent *C. auris* skin colonization across multiple sites for over a year. Persistent colonization is consistent with findings from our culture data, indicating that *C. auris* stably colonizes human skin, exhibiting particularly stable colonization at the nares (Extended Data Fig. 7).

Over the course of the study, nine residents who were initially colonized at one or more body sites cleared *C. auris* colonization across all body sites by the end of the study. For these nine residents, the proportion of samples dominated by *C. auris* (CST4) decreased from 16.0% to 0% (CST4) from the first to the third time point, while the proportion of sites dominated by *Malassezia* species (CST1) increased from 68.0% to 79.3%, respectively (Extended Data Fig. 8). In individuals who were persistently colonized, by contrast, the proportion of samples dominated by *C. auris* remained roughly constant over time (~30%). Communities that shifted away from *C. auris* toward *Malassezia* predominance experienced an increase in mycobiome diversity (Extended Data Fig. 9) and a reduction in proteobacterial abundances among the bacterial community in concert with the loss of *C. auris*. Clinically, transiently colonized residents were less likely to require mechanical ventilation or gastrostomy tubes than residents who were persistently colonized (χ^2, $P < 0.05$).

Collectively, these data suggest the resilience of the commensal skin communities to initial invasion. However, once *C. auris* establishes predominance in a community, it is capable of establishing persistent colonization of the skin.

Discussion

Here we integrate genomic, clinical and epidemiologic data, analyzing almost 4,000 samples from 57 residents over a 3-month period to investigate factors underlying persistent *C. auris*

colonization of residents of the ventilator ward of a skilled nursing facility with endemic *C. auris* and routine CHG bathing. Our investigation provides insights that can be applied to the design of potentially more effective programs to control *C. auris* transmission and prevent infections in long-term care settings, which bear a disproportionate burden of *C. auris* disease.

Colonization of sites not screened routinely may facilitate healthcare-associated transmission[17]. Screening of residents at high risk of *C. auris* carriage is typically carried out by collecting a composite bilateral axillae and inguinal creases swab sample. In our study, unilateral screening of axilla and inguinal crease would have detected only 35 of 57 colonized residents; we found that screening of six body sites was required to identify all colonized residents. The nares and palms and/or fingertips were colonized more frequently and carried higher bioburdens than other sites. While the inguinal creases and axillae were identified by Public Health England to be the two most persistently positive sites[18], a study conducted by the New York State Department of Public Health reported the sensitivity of anterior nares to be higher than that of composite axillae and inguinal creases[28]. Quantitative culture results of South Asian clade I from New York State and those of South American clade IV in our study are concordant, demonstrating higher bioburden in anterior nares than in axillae and/or inguinal creases for *C. auris*–colonized residents. Because sampling six body sites may not be practical for routine screening, targeting high-yield sites such as axillae and/or inguinal creases and anterior nares is still recommended. Modifying screening strategies to include additional body sites during intractable outbreaks may permit identification of reservoirs for intrafacility transmission. Investigating innovative specimen collection methods, such as using sponge swabs to sample larger areas of skin[29], may also be of benefit. Frequent and dense colonization of anterior nares and palms and/or fingertips suggests that nasal decolonization and promotion of resident hand hygiene may be options to help reduce cross-transmission of *C. auris* in skilled nursing facilities. Finally, the imperfect sensitivity of most screening methods highlights the importance of universal, facility-wide infection-prevention measures, such as healthcare provider hand hygiene and environmental disinfection, in reducing *C. auris* transmission.

Despite the apparent susceptibility of *C. auris* isolates to CHG in vitro, the odds of recovering *C. auris* from skin sites by culture were reduced only at high measured concentrations of CHG. It is notable that the nares, a site not subject to CHG bathing, and the body sites with the lowest average concentration of CHG (palms and/or fingertips and toe webs) were frequently and densely colonized with *C. auris*. Heterogeneity in CHG concentration may have been due to differences in time since the last CHG bath, a variable not recorded by ventilator-capable skilled nursing facility personnel. Relatively high concentrations of CHG observed in inguinal samples may result from increased focal bathing as part of incontinence care. Nevertheless, our finding that only 7.3% of samples had concentrations of CHG sufficiently high to be associated with reduced odds of *C. auris* colonization suggests that a point of intervention may be ensuring that all skin sites maintain high residual concentrations of CHG[10]. We were encouraged to find no evidence of an association between CHG concentration and perturbation of the commensal skin microbiome.

Persistent *C. auris* colonization reported here is consistent with observations of several patient and resident populations in acute and long-term care settings, respectively[3,18], including another facility with routine CHG bathing[9]. Our analysis of mycobiome dynamics suggests that commensal, *Malassezia*-predominated communities are resilient to invasion by *C. auris*. By contrast, we observed that *C. auris* predominance is relatively stable once it occurs, with a 30–50% chance that *C. auris* will persist at sites once it comes to dominate. The ascension of *C. auris* to dominance in the community appeared to occur through an intermediate state (CST2) in which diverse *Candida* spp. co-predominate skin sites with a ~40% probability that sites would transition from the diverse *Candida* state toward *C. auris* predominance. This finding is consistent with prior work demonstrating that *C. auris* has a higher predilection for skin colonization than does *C. albicans*[6,30], which in turn is a better skin colonizer than *C. tropicalis* or *C. parapsilosis*[26].

Our observation that a community of diverse *Candida* species is an intermediate state between commensal *Malassezia* and *C. auris* predomination provides an additional possible point of intervention for infection prevention. While we did not examine the in vitro susceptibility of *Malassezia* spp. to CHG, microbiome sequencing results failed to provide evidence of a linear relationship between CHG concentration and the abundance of *Malassezia* spp. Selection of *C. auris* by CHG bathing is one possible explanation for the high transition rate to *C. auris* predominance. However, countering this argument is our observation that *C. auris* was more stable at the nares, a site not subjected to CHG bathing, as compared to sites undergoing bathing. Our analysis revealed a variety of Gram-negative bacterial species commonly found in nursing home settings, including *P. aeruginosa*, *P. mirabilis*, *K. pneumoniae* and *P. stuartii*, to be enriched in *C. auris*–positive samples. However, due to the widespread prevalence of *C. auris* in the facility at the outset of the study and complex medical histories of these residents, we could not determine whether the bloom of Gram-negative species preceded *C. auris* colonization or vice versa, nor could we determine the temporal relationship between antibiotic receipt and colonization with these Gram-negative bacteria or *C. auris*. Similarly, our study design precluded determination of whether associations of *C. auris* colonization with other clinical covariates, such as mechanical ventilation, reflect merely the generally poorer health of colonized residents or are causally related to colonization. Elucidating the effect of antibiotic exposure on skin microbial communities and *C. auris* colonization and dominance is of particular importance, as this risk factor may be modifiable. Exposure to a carbapenem, vancomycin or fluconazole was associated with increased odds of *C. auris* colonization in another recent study of long-term care residents[31].

One limitation of this study is that the different clades of *C. auris* may exhibit different body-site tropisms; therefore, our results may not be generalizable to colonization with *C. auris* other than South American clade IV. The single-center setting of our study also may reduce its generalizability. Sample collection for this work began after prevalence at the facility reached saturation, making it difficult to understand patterns of diversity in the microbiome before the intro- duction of *C. auris*. To gain insight into how antibiotic-mediated reductions in colonization resistance might increase risk of colonization, future work should aim to disambiguate the onset of these effects in other healthcare settings. Finally, our experimental design enabled quantification of CHG concentrations across body

sites but lacked a comparator group against which we could assess the impact of CHG bathing as a controlled intervention.

Our data suggest that residents of ventilated skilled nursing facilities where *C. auris* is endemic and CHG bathing is routine have highly personalized patterns of *C. auris* skin colonization. This site-to-site variability in colonization limits infection-control strategies predicated on targeting only known *C. auris*–colonized individuals; facility or unit-wide infection-control approaches may be more effective. We found that perturbation of the skin micro- biome is a potential risk factor for *C. auris* colonization and per- sistence. These data have implications not only for facilities where *C. auris* is endemic but also for other facilities embedded within the same regional healthcare networks[32]. While *C. auris* outbreaks in the United States have been reported primarily in long-term care settings, a recent report of a *C. auris* outbreak in a coronavirus disease 2019 (COVID-19) specialty care unit highlights the threat that *C. auris* poses to acute care hospitals[33]. Our findings have identified candidate targets for future interventions related to skin microbiome dynamics, including the potential for preserving or restoring commensal skin microbiota to augment existing approaches for *C. auris* control.

Online content

Any methods, additional references, Nature Research reporting summaries, source data, extended data, supplementary information, acknowledgements, peer review information; details of author contributions and competing interests; and statements of data and code availability are available at https://doi.org/10.1038/s41591-021-01383-w.

Methods

Participant recruitment.

This research complies with all relevant ethical human research regulations. The study was reviewed and approved by the Rush University Institutional Review Board, which granted expedited review and waiver of informed consent. Study participants did not receive monetary compensation for their participation. Demographics of the participant population are reported in Table 1.

Statistics and reproducibility.

We conducted an observational, serial cross-sectional study of residents of a ventilator-capable skilled nursing facility (vSNF) in Chicago, IL, USA. All residents on the 70-bed ventilator ward of the 300-bed vSNF at the time of the first survey were eligible for study participation. Although this work was exploratory, we conducted an a priori power analysis to ensure that we would have sufficient power to detect notable differences in the prevalence of *C. auris* colonization at different body sites, that is, to test the null hypothesis of uniform distribution of *C. auris* across body sites. When we were planning the study, we anticipated participation of 35 residents with *C. auris* colonization and 25 residents without *C. auris* colonization during the three serial point prevalence surveys. We based these estimates on documented incidence, prevalence and turnover rates at that time and an assumption of 80% resident participation. Assuming participation of 35 *C. auris*–colonized residents, true

positive rates at the reference site ranging from 70% to 90% and $\alpha = 0.05$, we calculated that we would have 80% power to detect relative risk in any comparison site ranging from 0.62 to 0.75, that is, 44–68%. In fact, we identified 45 *C. auris*–positive residents and 12 *C. auris*–negative residents during the first survey. Therefore, rather than seeking new residents to test during each of the subsequent two surveys, we continued to follow the original 57-resident cohort, eventually identifying a total of 49 residents who were ever positive for *C. auris* and eight residents who were never positive for *C. auris*.

Statistics on clinical variables describing the study cohort.

Odds ratios and two-tailed *P* values for continuous variables (that is, length of stay before the first swab, age, Charlson comorbidity index and Braden score) were determined using binary logistic regression analyses with *P* values determined by Wald χ^2 statistics. For dichotomous variables, two-tailed *P* values were determined from Fisher's exact tests. To calculate an odds ratio for mechanical ventilation and antifungal receipt in the prior 90 d, where the values in the 'not colonized' group are 0, logit estimates were used, in which a correction of 0.5 was added to each cell in the table. None of the *P* values for clinical analyses were adjusted for multiple comparisons.

Estimating the proportion of colonized residents by body sites.

The proportion of colonized residents was calculated as previously described[34]. Exact binomial 95% confidence intervals were calculated using the 'epi.tests' function in the 'epiR' package.

Estimating sensitivity of sites for identifying colonized residents.

We used a custom function leveraging the 'combn' function in base R and the 'epiR' package to generate the 'proportion of colonized individuals' for all possible two-way ($n = 45$), three-way ($n = 120$), four-way ($n = 210$), five-way ($n = 252$), six-way ($n = 210$), seven-way ($n = 120$), eight-way ($n = 45$) and nine-way ($n = 10$) groupings of the ten body sites. Sensitivity was computed by dividing the 'proportion of colonized individuals' by the proportion of residents positive at any body site.

Estimating bioburden of *C. auris* across body sites.

Flocked swabs (FLOQSwabs, Copan) were used to sample a 5×5 cm^2 area from each body site and were placed immediately in Amies medium with neutralizer without ether sulfate[35,36]. Aliquots (100 µl) were inoculated directly onto CHROMagar Candida plates (Becton Dickinson) and incubated at 37 °C for 7 d. A second 100-µl aliquot was inoculated into Salt Sabouraud Dulcitol Broth and incubated at 40 °C for 7 d; cloudy broth cultures were subsequently inoculated onto CHROMagar Candida plates[37] and incubated for 7 d. Each unique colony morphology underwent identification to the species level by MALDI-TOF (VITEK MS Plus (bioMérieux). Resulting CFU from directly inoculated plates for all colonized sites (excluding uncolonized sites) at the first time point were plotted with the 'geom_density_ridges' function in the package 'ggridges'.

Axilla, inguinal crease and anterior nare samples were also processed with an MPN method that tested eight serial dilutions of the original sample with the enrichment broth

method. Three replicates were performed for each dilution, enabling calculation of an MPN as described at https://www.fda.gov/food/laboratory-methods-food/bam-appendix-2-most-probable-number-serial-dilutions. High-throughput-format MPN analysis was performed using 96-well 2-ml deep-well blocks in which 500-µl volumes of Sabouraud broth with dulcitol, chloramphenicol and gentamicin were inoculated with 50-µl sample aliquots from each replicate for each dilution. Culture blocks were incubated at 40 °C for 7 d before plating onto CHROMagar Candida plates in 10-µl volumes. Plates were checked for growth after 7 d. Growth with morphology characteristic of *C. auris* was confirmed for both culture methods to the species level using MALDI-TOF.

CHG and antifungal susceptibility testing and determination of the CHG concentration on skin.

To determine the CHG concentration on skin, swabs (Bio-Swab, Arrowhead Forensics) moistened with sterile water were used to sample areas of skin adjacent to those areas that were sampled for culture and microbiome analysis, only at sites bathed routinely with CHG. CHG concentrations were measured using a quantitative colorimetric method that was read by visual inspection as described previously[38].

CHG susceptibility was determined using a yeast broth microdilution method in accordance with CLSI guidelines[39,40], starting with a 20% solution of chlorhexidine digluconate (Sigma). Susceptibility to selected antifungal agents was determined using a commercial microdilution method (Sensititre YeastOne YO9 AST Plate, Thermo Scientific) and applying tentative breakpoints published by the CDC[41].

Association of CHG concentration with *C. auris* colonization.

Mixed-effects regression models were used to control for clustering of body sites within residents over time. For CHG concentration by body site, a mixed-effects ordinal logistic regression model was used. For testing the relation between CHG concentration ($\log_2$ transformed) and *C. auris*, a series of mixed-effects binary logistic regression models was used. The first model tested the linear relation between CHG concentration and *C. auris* colonization ($\log_2$ transformed), controlling for body site. This was followed by a series of ten models testing cutoff points for CHG concentration at each successive increment in the semiquantitative test for CHG concentration.

Microbiome sample collection, DNA extraction, PCR amplification and sequencing.

Swab samples from each anatomic site were collected (Extended Data Fig. 1) using our previously published protocols; negative controls were also collected and subsequently processed in parallel with true samples as described previously[42]. Briefly, foam swabs (Puritan, 2515061PF) were premoistened with Yeast Cell Lysis solution (Lucigen) and used to collect swab samples from the skin across individual sites that were adjacent to sites sampled for culture and CHG-concentration measurement. Swabs were stored in lysis solution at −80 °C following collection. For extraction, skin swabs were incubated in Yeast Cell Lysis buffer and Ready-Lyse Lysozyme solution (Lucigen) for 1 h with shaking at 37 °C. Steel beads (5 mm) were added to mechanically disrupt fungal cell walls using a TissueLyser (Qiagen) for 2 min at 30 Hz, followed by 30-min incubation at 65 °C

for complete lysis. MPC reagent was added to samples, and resulting supernatants were processed using the PureLink Genomic DNA kit (Invitrogen). DNA was eluted in DNA-Free PCR Water (Qiagen).

The ITS1 region was amplified using primers modified with Illumina adaptors 18S-F (5′-GTAAAAGTCGTAACAAGGTTTC) and 5.8S-1R (5′-GTTCAAAGAYTCGATGATTCAC) as previously described[43,44]. The following PCR conditions were used: 2.5 μl 10× PCR buffer, 4 μl dNTP mix, 0.25 μl Takara LA Taq Polymerase (Clontech), 1 μl 18S-F (10 μM), 1 μl 5.8S-1R (10 μM), 13.75 μl PCR Water (Qiagen) and 2.5 μl DNA. Reactions were performed in duplicate for 30 cycles, combined, purified using the Agencourt AMPure XP system (Beckman Coulter) and quantified using the Quant-iT dsDNA kit (Invitrogen). Equivalent amounts of amplicons were pooled together, purified with the MinElute PCR purification kit (Qiagen) and sequenced on an Illumina MiSeq. The V1–V3 region of the bacterial 16S gene was amplified under similar conditions using primers 27F (5′-AGAGTTTGATCCTGGCTCAG) and 534R (5′-ATTACCGCGGCTGCTGG).

Demultiplex and quality filtering of amplicon tables.

A total of 5.3×10^7 raw reads were analyzed for 16S amplicons, while a total of 1.47×10^7 raw reads were analyzed for the ITS1 table. Forward and reverse reads were independently demultiplexed, and sequences were parsed into sample-specific files with Illumina's 'bcl2fastq' version 2.20 software; primers were trimmed from sequences using cutadapt 2.10* before import into R 3.6.1 for quality filtering with the R package 'dada2'; the 'filterAndTrim' function was used to truncate reads at the first instance of a quality score of 2 before elimination of reads with more than 0 ambiguous characters, a maximum expected error exceeding 2 or a length less than 50 nucleotides. Error rates were learned independently on filtered forward and reverse reads using default parameters before dereplication, inference of sequence-specific errors (with self-consistency set to true and pooling set to true) and elimination of problematic reads. Dereplicated and filtered forward sequences were subsequently merged with their paired-end reads before construction of an amplicon sequence variant (ASV) table. The 'removeBimeraDenovo' function of dada2 set to the 'consensus' method was used to filter chimeras from each ASV table. Taxonomic assignment was then performed down to the species level when possible using the dada2 implementation of the RDP Naive Bayesian Classifier 3 trained on the RefSeq database version 2.0 downloaded in May 2018 for bacterial reads and the UNITE 'sh_general_release_dynamic' database downloaded on 2 February 2019. Datasets generated as direct output from dada2 are referred to as 'merged_16s' and 'merged_ITS', and sequencing depths associated with these tables were 12,466,948 (16S) and 39,481,121 (ITS).

Quality control of the sequence tables.

To deplete taxa enriched in extraction controls and therefore likely associated with contamination, a data subset was generated, consisting only of the technical controls (16S, $n = 150$; ITS, $n = 90$), which were sequenced in parallel with true samples (16S, $n = 1,258$; ITS, $n = 1,318$). An enrichment score was calculated for enrichment of taxa in controls compared to samples and vice versa; taxa enriched in controls relative to samples were

deleted from the dataset as previously described[45]. Filtering using this method reduced the 16S table to 854 taxa across 1,243 samples and the fungal table to 136 taxa across 1,226 samples. Reads were agglomerated to the taxonomic rank of species using the 'tax_glom' function of 'phyloseq'. Subsequent to taxonomic agglomeration, samples with fewer than 500 reads per sample were dropped. Finally, samples were dropped from the 16S table if the ITS1 sample failed quality control, generating sample sets of equal size (n = 1,152) across 'bac_match' and 'its_match' datasets.

Identifying bacteria associated with colonization.

To reduce the influence of highly variant taxa on findings, species present in fewer than 20% of 16S samples were dropped. Reads were subsequently transformed using centered-log-ratio transformation as implemented in the 'compositions' package. The 'splsda' function of the 'mixomics' package was used to identify bacterial species positively or negatively associated with *C. auris* culture.

Community state type analysis.

The weighted UniFrac statistic was computed on *Malassezia* and *Candida* species with the distance function of 'phyloseq' before performing independent rounds of cluster analysis from one to 30 clusters using the 'partition around medoids' function of the 'cluster' package. The gap statistic was computed for each cluster analysis from one to 30 using the 'clusGap' function and 1,000 Monte Carlo bootstrap samples. To evaluate the robustness of the identification of four clusters in the data, this process was repeated using the Bray–Curtis dissimilarity metric. The four clusters for the weighted UniFrac analysis were subsequently labeled as CSTs.

Markov chains.

A data subset was generated in which only samples from 23 residents who had a complete set of survey 1 and survey 2 samples at the fingertips, toe webs, nares and inguinal crease were retained. Based on prior work[46], a custom function was written to generate the initial state matrices from the phyloseq S4 object 'its_match'. Transition matrices were obtained with a custom function that standardized each initial state matrix to four rows and four columns before normalization to row sums. Missing values, corresponding to states that were not observed at a given site, were replaced with 0. Each transition matrix was subsequently used as input for the new 'markovchain' function of the 'markovchain' package. Predictions for N-month time points were obtained by multiplying the initial state matrix by the transition matrix raised to the Nth power. Each transition matrix was visualized using a custom function leveraging the 'plotmat' function in the 'diagram' package.

Illumina whole-genome sequencing.

Isolates of *C. auris* (various clades) were streaked onto CHROMagar Candida plates (BD, 254093) and incubated at 37 °C for 24–48 h. Colonies were transferred to 600 μl Yeast Cell Lysis buffer (Lucigen, MPY80200) with 3 μl RNase (Qiagen, 19101) and 1-mm glass beads (MP Biomedicals, 116912050-CF). Cells were subjected to bead beating in a FastPrep 5G

(MP Biomedicals) at speed 6.5 for 15 s and placed on ice for 1 min, and the procedure was repeated. The cell lysate was incubated at 65 °C, and the protocol continued as directed (Lucigen, MPY80200). The genomic DNA pellet was resuspended in 0.1× TE, pH 8.0. Libraries were generated from genomic DNA with the Nextera XT Library Preparation kit (Illumina) as per the manufacturer's recommendations. Libraries were pooled at an equimolar ratio for sequencing on the Illumina NovaSeq 6000 to obtain a minimum of 2.6 million 151-bp reads per individual library. Illumina sequence data were processed using RTA version 3.4.4.

Nanopore sequencing and assembly.

A fraction of genomic DNA prepared for lllumina whole-genome sequencing was reserved for nanopore sequencing and assembly. Genomic DNA was assessed by Femto Pulse (Agilent) analysis and determined to be approximately 15 kb; therefore, shearing was not performed. A library was prepared for long-read Oxford Nanopore Technologies (ONT) sequencing from 1 μg DNA using the Ligation Sequencing kit (ONT, SQK-LSK109). Twenty fmol of the library was sequenced on an R9 flow cell using the ONT GridION platform running MinKNOW 3.6.5 and run for 72 h with refueling at 48 h. Guppy 3.6.0 was used to convert raw sequence data files to basecall fastq files. A total of 13.0 Gb of data was collected with an N50 length of 14.3 kb and a mean read length of 11.4 kb. ONT sequence reads were randomly downsampled to an estimated 200× coverage using 'seqtk' version 1.2 (https://github.com/lh3/seqtk) and assembled using Canu 2.0 (ref. [47]). Assembled contigs were polished with the ONT sequence reads for one round using Racon version 1.3.1 (ref. [48]), followed by two rounds with medaka version 1.0.3 (https://github.com/nanoporetech/medaka). Contigs were polished further by aligning Illumina short reads using Bowtie 2 version 2–2.4.2 (ref. [49]) and running Pilon version 1.23 (ref. [50]) on the alignment file.

Variant calling.

Illumina NovaSeq reads for each of four outbreak isolate genomes were aligned to the nanopore reference genome, and single-nucleotide variants were identified with snippy version 4.4.1 (https://github.com/tseemann/snippy) with default options deploying BWA version 0.7.17 and FreeBayes version 1.3.5 algorithms, requiring a read depth of at least 10× and the additional flag '–minfrac 0.9', requiring at least 90% of reads in support of the variant nucleotide call. SAMtools (version 1.11) coverage was used to estimate coverage and mapping quality across the genomes of isolates (mean coverage, 99.99; mean MAPQ score, 59.6).

Reporting Summary.

Further information on research design is available in the Nature Research Reporting Summary linked to this article.

Data availability

Sequencing data are publicly available in the NIH Short Read Archive under BioProject accession number PRJNA672955. The RefSeq database version 2.0 downloaded on May 2018 and the UNITE 'sh_general_release_dynamic' database downloaded on 2 February

2019 were used to assign bacterial and fungal taxonomy, respectively, and can be found at https://github.com/skinmicrobiome/cauris_colonization. Intermediate data files including the OTU table, the taxonomy table and the sample data mapping file are included in Supplementary Data 1.

Code availability

The R code used to generate figures is provided in Supplementary Data 2–5 and can be found at https://github.com/skinmicrobiome/cauris_colonization.

Extended Data

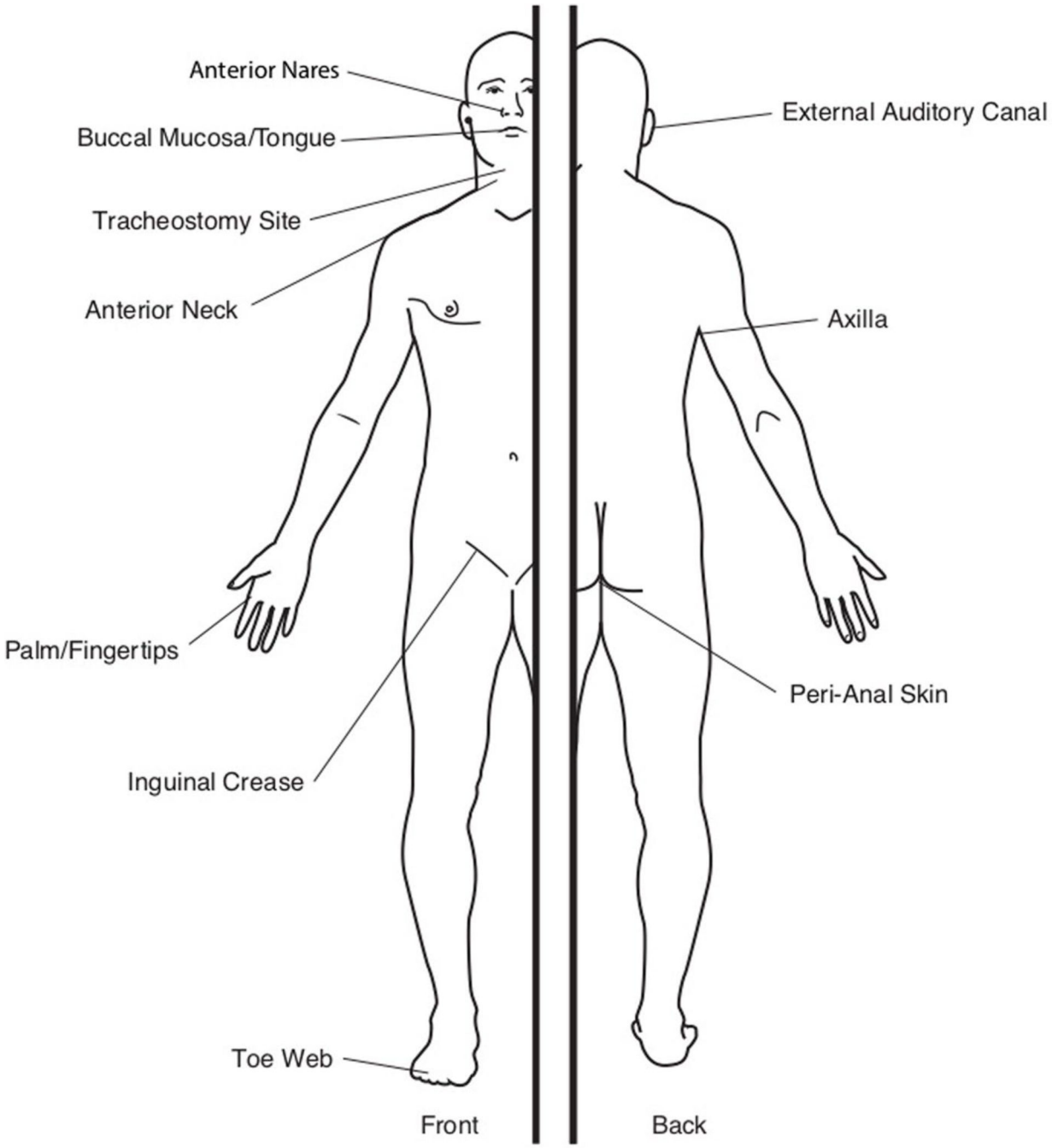

Extended Data Fig. 1 |. Map of sample sites.
We surveyed 10 body sites per subject, including the anterior nares (N), tracheostomy site (Tc), anterior neck (Ne), palms/fingertips (Fg), buccal mucosa/tongue (Bu/To), inguinal crease (Ic), axilla (Ax), toe web (Tw), external auditory canal (Ea), and peri-anal skin (An).

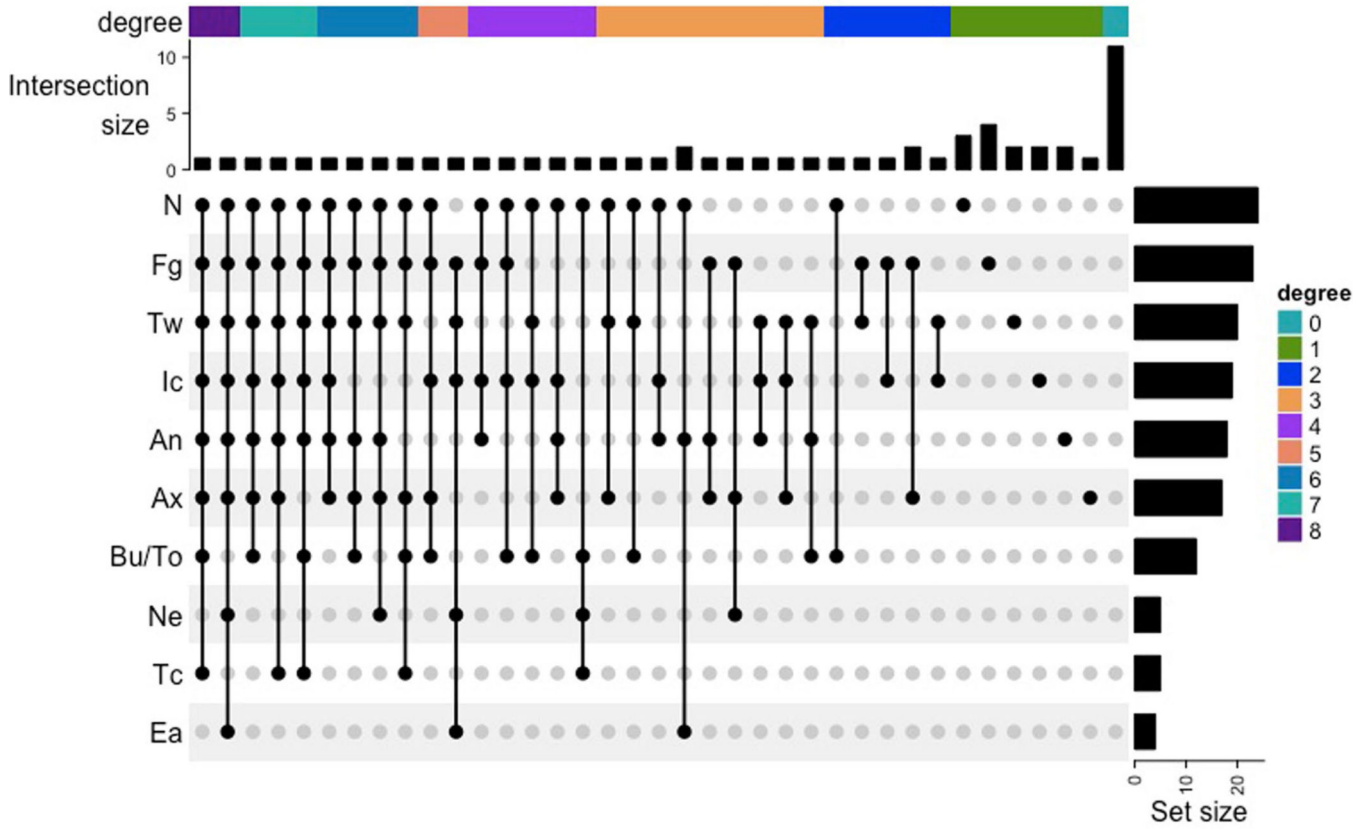

Extended Data Fig. 2 |. Patterns of body site colonization visualized with UpSetR.

Colors map to degree, a measure of the number of co-colonized sizes. A total of 36 distinct co-colonization patterns were observed, each arranged from the left to the right as a function of decreasing degree. The intersection size is the number of subjects whose body-site colonization matches the points connecting sites for each of the 36 unique co-colonization patterns. For example, the nares (N) and fingertips/palm (Fg) are more frequently mono-colonized than any of the other sites while the buccal mucosa/tongue (Bu/To), neck (Ne), tracheostomy site (Tc), and external auditory canal (Ea) are never mono-colonized. Most patients have a distinct pattern of co-colonization with the most frequent pattern being singular colonization of the nares (N) or fingertips/palm (Fg). The set size corresponds to the frequency of colonization for each site for the first time point.

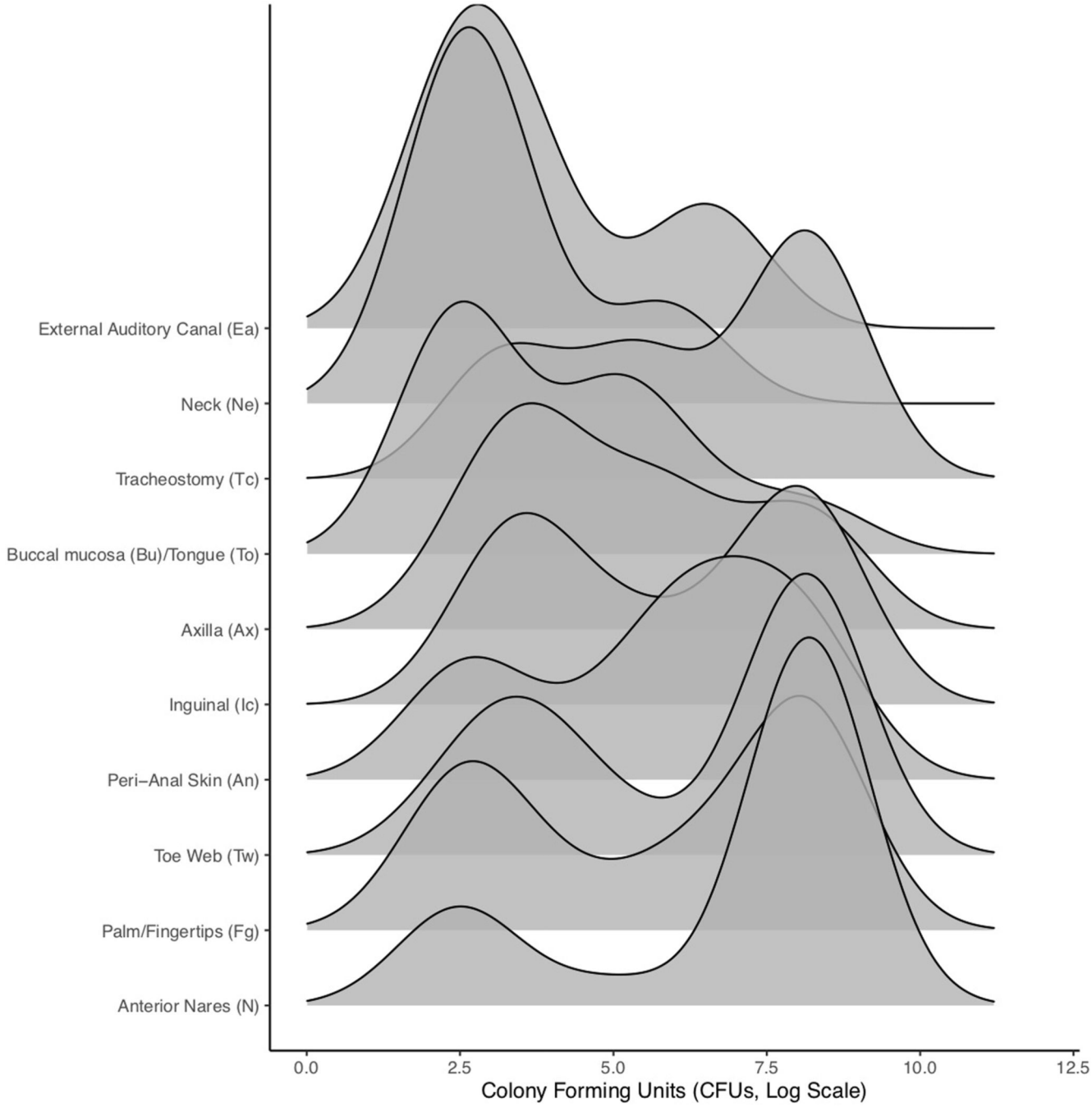

Extended Data Fig. 3 |. Ridgeline plot of sample colony counts for each site during the first survey.

The cumulative distribution for each ridgeline sums to 1, with peaks corresponding to peak bioburden (log colony forming units), for each site. For any given site, a bimodal distribution indicates a subset of subjects shared relatively high bioburdens and another a subset of subjects shared relatively low bioburdens. Sites with low level colonization include the external auditory canal and neck while sites having the highest bioburden include nares and inguinal crease.

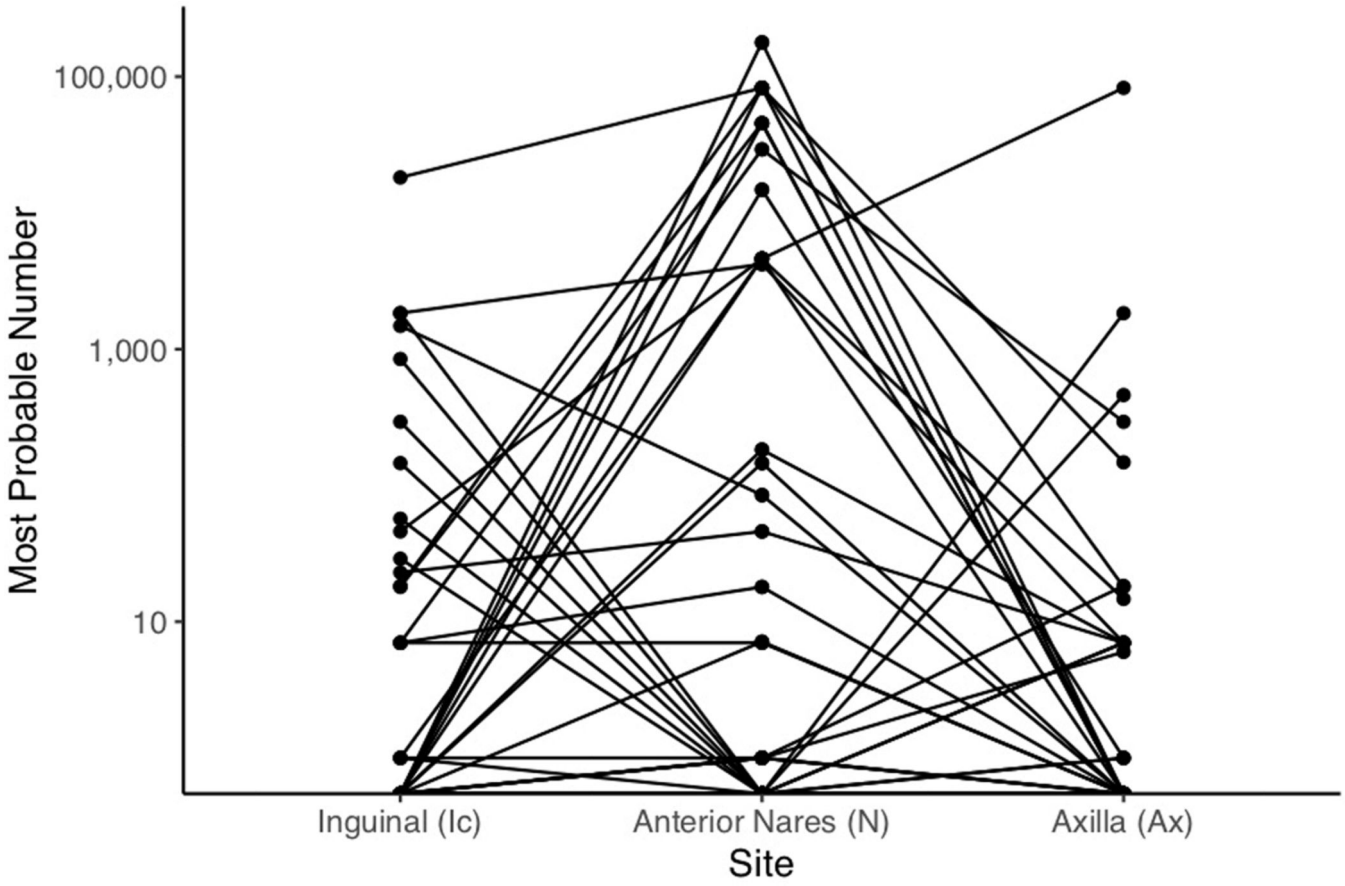

Extended Data Fig. 4 |. Paired Most Probable Number (MPN) Analysis.

MPN estimates are shown for the inguinal crease, anterior nares, and axilla. Data represented are from the first point prevalence survey. Each line represents an individual. Individual trajectories reveal a large number of individuals with high counts at the nares and either absent or low-level colonization at the axilla or inguinal crease.

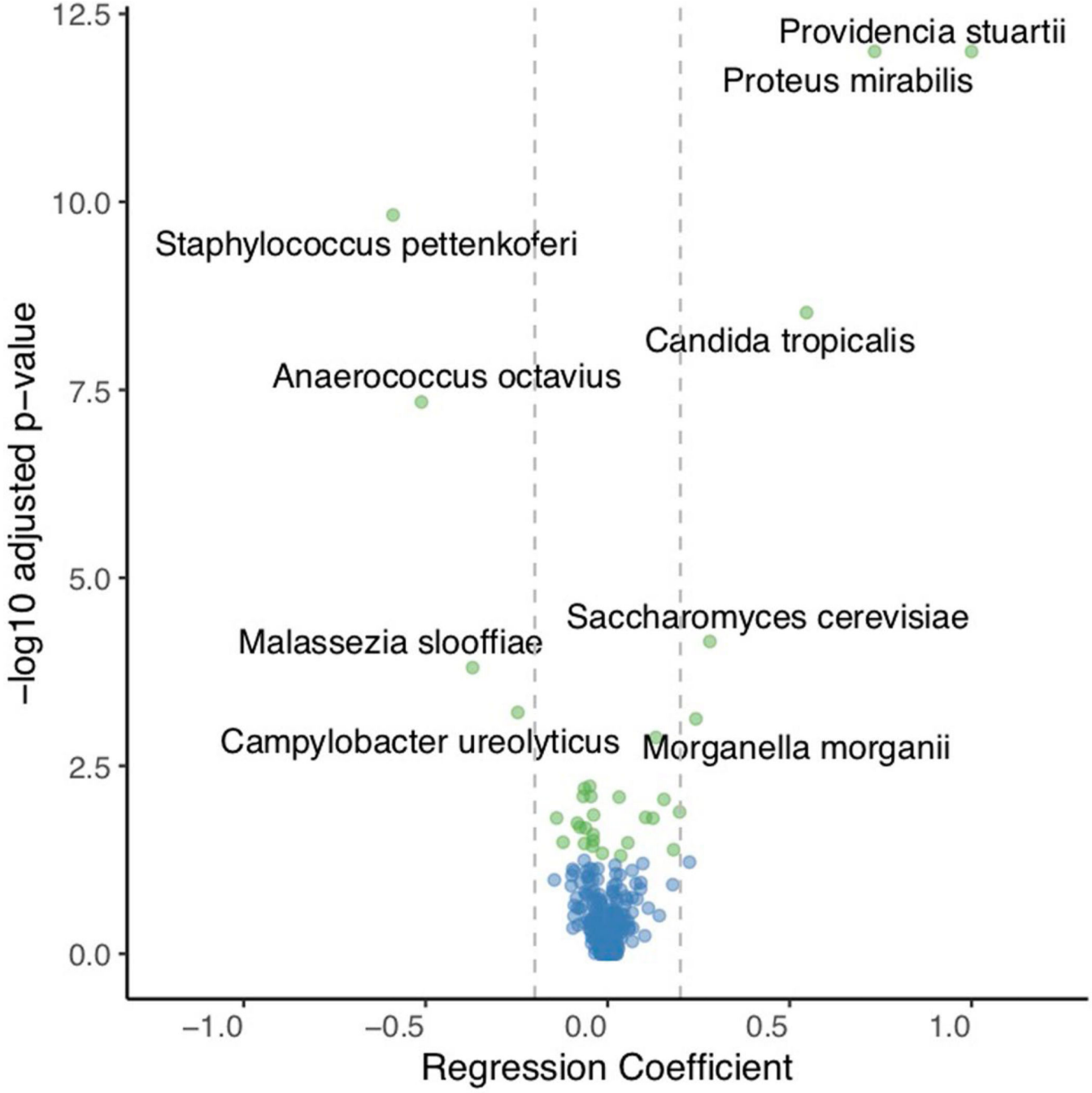

Extended Data Fig. 5 |. Volcano plot of statistical significance (-Log adjusted p-value) against the regression coefficients from linear mixed effects models.

Each point represents a regression coefficient for a bacterial or fungal species. The vertical lines demarcate regression coefficients of −0.2 and 0.2. Species having Holm adjusted p-values < 0.05 are highlighted in green while non-significant taxa are in blue. Species exhibiting a positive association with CHG concentration (skin concentrations (estimate > 0.2, Holm adjusted $p < 0.05$) include *Providencia stuartii, Proteus mirabilis, Candida tropicalis, Saccharomyces cerevisiae* and *Morganella morganii*. Species exhibiting a negative correlation with CHG skin concentrations (estimate < −0.2, Holm adjusted $p < 0.05$)

include *Staphylococcus pettenkoferi, Anaerococcus octavius, Malassezia slooffiae*, and *Campylobacter ureolyticus*.

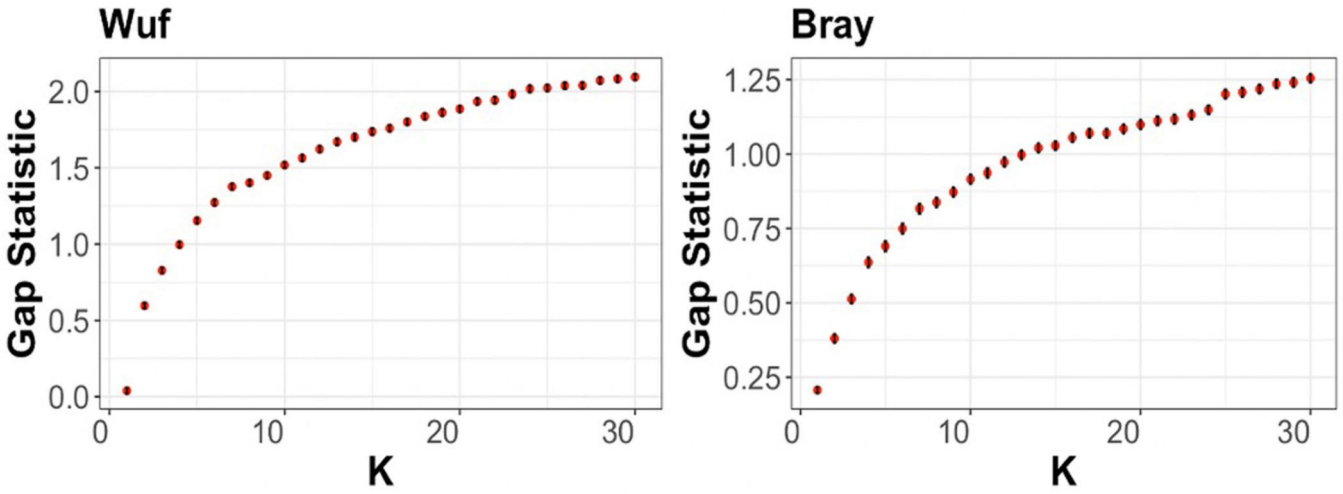

Extended Data Fig. 6 |. Evaluation of the robustness of cluster formation.
Weighted UniFrac (Wuf) and Bray-Curtis (Bray) distances were computed prior to partition around medoids analysis. The gap statistic (y-axis) is plotted as a function of K (x-axis), defined as the number of clusters evaluated. The error bars correspond to the confidence interval generated on 1000 bootstraps. The optimal number of clusters corresponds to K where additional clusters fail to increase the gap statistic using both a phylogenetically aware distance metric (UniFrac) and Bray Curtis.

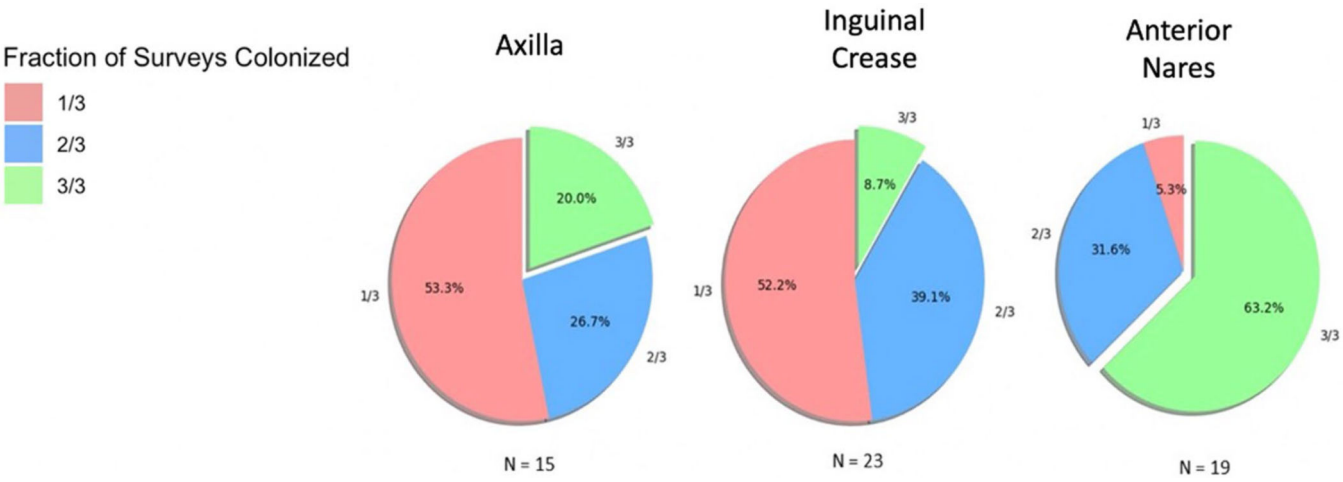

Extended Data Fig. 7 |. Temporal stability of *C. auris* colonization at the axilla, inguinal crease and anterior nares.
Patients who were qualitatively categorized as positive at least once, based on MPN data, were categorized as positive in 1 of 3 (pink), 2 of 3 (blue) or 3 of 3 (green) surveys. The majority of subjects colonized at axilla and inguinal crease were positive in 1/3 surveys while the majority of individuals colonized at the nares were positive at all 3 surveys.

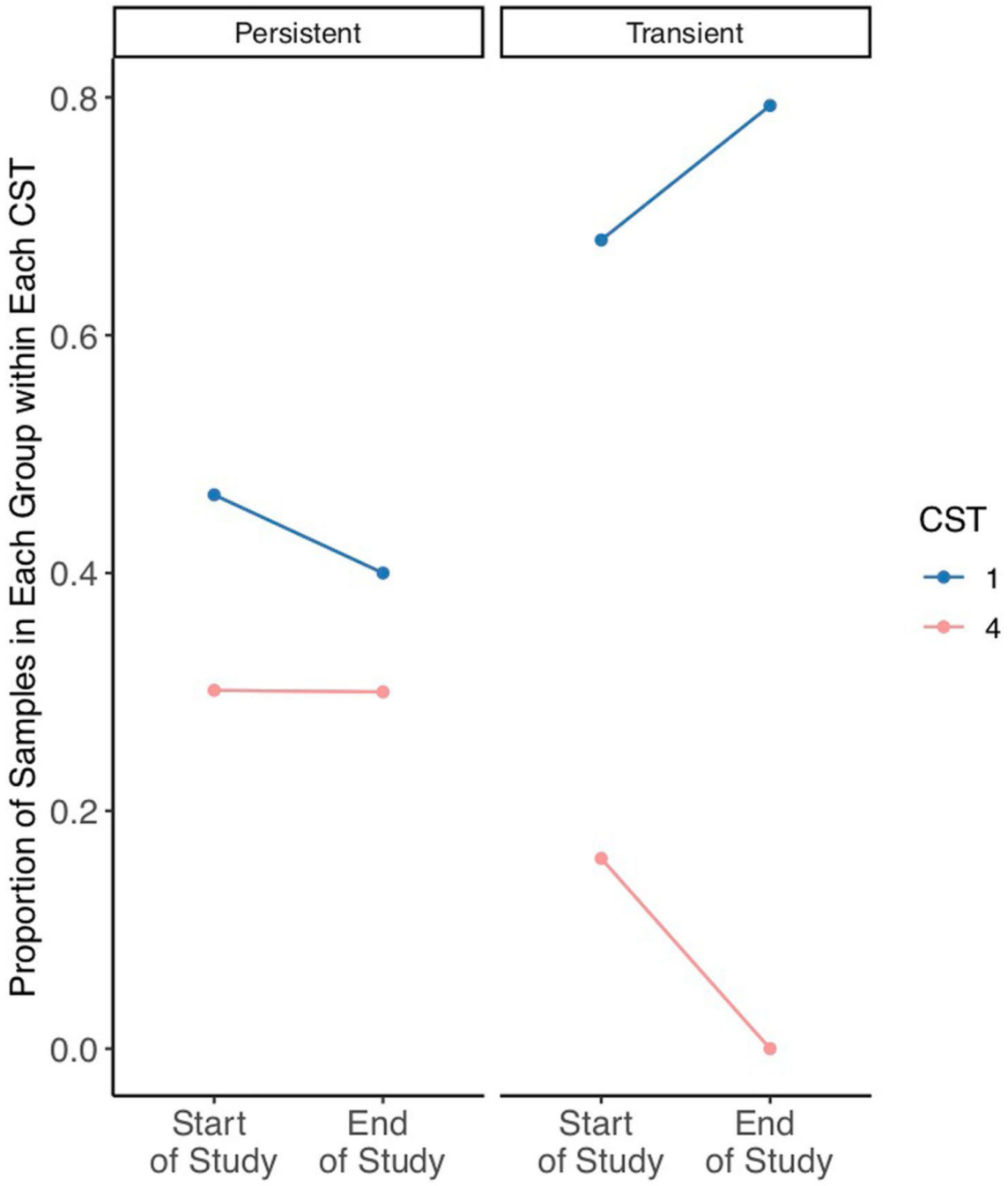

Extended Data Fig. 8 |. Proportion of sites within each CST over time for individuals who were either transiently or persistently colonized.

The proportion of samples dominated by *C. auris* (CST4) remained roughly constantly (~30%) for individuals who were persistently colonized (Left). In contrast, the proportion of sites dominated by *C. auris* dropped from 16% to 0% from the first to the third time point in transiently colonized individuals (Right). Among those transiently colonized, the reduction in sites dominated by *C. auris* was accompanied by a concomitant increase in the proportion of sites dominated by commensal Malassezia species. Of special interest, the proportion of

sites dominated by Malassezia species was higher across all time points for those who were transiently colonized compared to those persistently colonized.

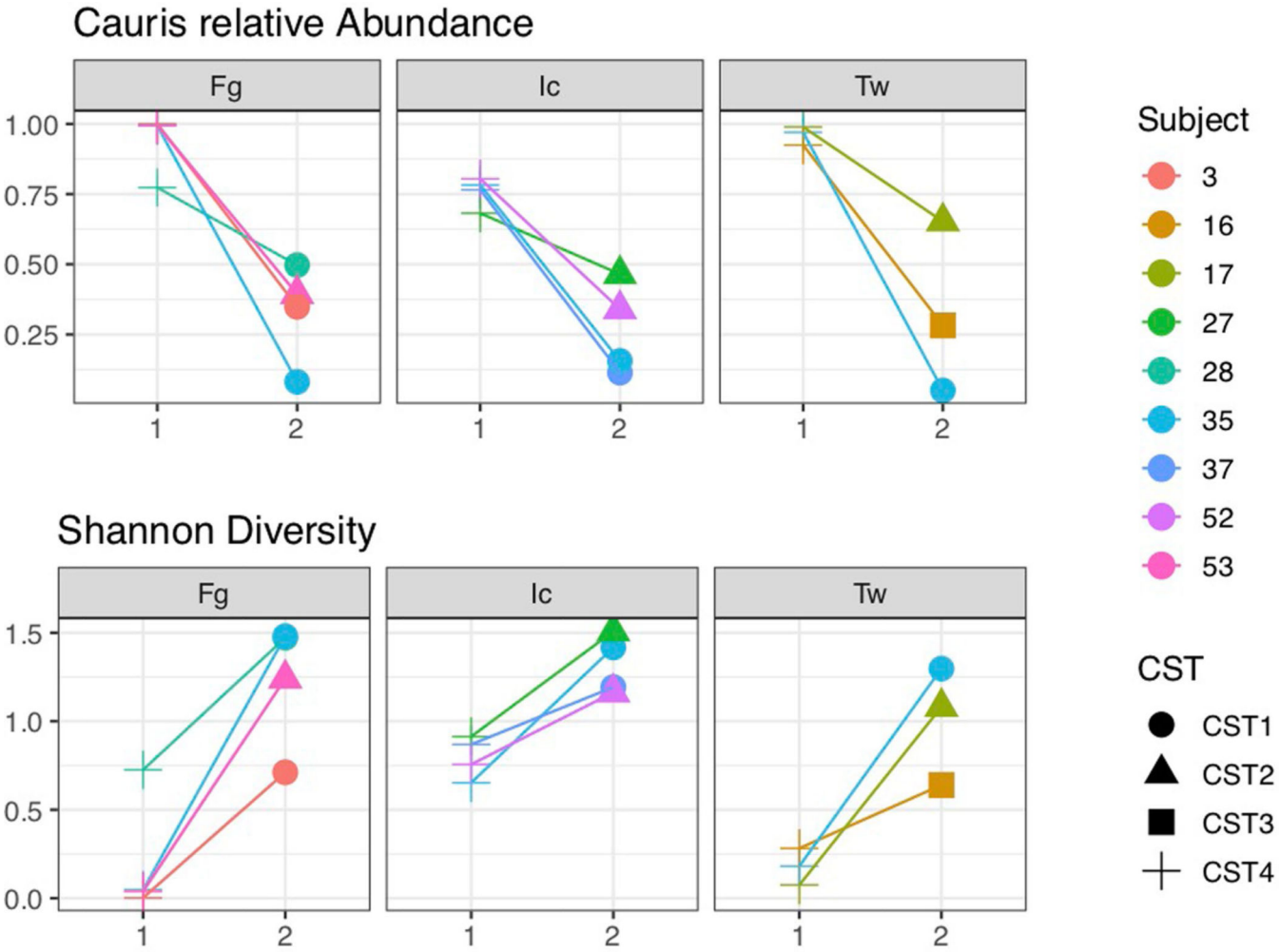

Extended Data Fig. 9 |. Examination of the mycobiome at sites that transition away from *C. auris* domination between survey 1 and survey 2.

Colors correspond to unique subjects. Shapes correspond to the mycobiome CST. Across all panels, survey 1 or 2 is shown on the x-axis. On the y-axes, the relative abundance of *C. auris* (top panel) or Shannon diversity (bottom panel) is depicted. For this analysis we looked exclusively at sites that transitioned away from domination by *C. auris* at the first survey (Survey 1) towards domination by another species at the second time point (Survey 2).

Supplementary Material

Refer to Web version on PubMed Central for supplementary material.

Acknowledgements

The findings and conclusions in this report are those of the authors and do not necessarily represent the official position of the CDC. This work was supported in part by CDC contract number 75D30118C02900. This study used the computational resources of the National Institutes of Health (NIH) HPC Biowulf Cluster (http://hpc.nih.gov). This work was supported by the Intramural Research Programs of the NIH National Institute of Arthritis and Musculoskeletal and Skin Diseases and the National Human Genome Research Institute. We thank J. Fekecs for assistance rendering publication-ready figures.

References

1. Jeffery-Smith A et al. *Candida auris*: a review of the literature. Clin. Microbiol. Rev. 31, e00029–17 (2018). [PubMed: 29142078]
2. Tsay S et al. Notes from the field: ongoing transmission of *Candida auris* in health care facilities —United States, June 2016–May 2017. MMWR Morb. Mortal. Wkly Rep. 66, 514–515 (2017). [PubMed: 28520710]
3. Vallabhaneni S et al. Investigation of the first seven reported cases of *Candida auris*, a globally emerging invasive, multidrug-resistant fungus—United States, May 2013–August 2016. Am. J. Transplant. 17, 296–299 (2017). [PubMed: 28029734]
4. Chen J et al. Is the superbug fungus really so scary? A systematic review and meta-analysis of global epidemiology and mortality of *Candida auris*. BMC Infect. Dis. 20, 827 (2020). [PubMed: 33176724]
5. Centers for Disease Control and Prevention. Antibiotic Resistance Threats in the United States, 2019 (US Department of Health and Human Services, CDC, 2019). .
6. Horton MV et al. *Candida auris* forms high-burden biofilms in skin niche conditions and on porcine skin. mSphere 5, e00972–19 (2020). [PubMed: 31969480]
7. Weschler CJ et al. Squalene and cholesterol in dust from Danish homes and daycare centers. Environ. Sci. Technol. 45, 3872–3879 (2011). [PubMed: 21476540]
8. Biswal M et al. Controlling a possible outbreak of *Candida auris* infection: lessons learnt from multiple interventions. J. Hosp. Infect. 97, 363–370 (2017). [PubMed: 28939316]
9. Schelenz S et al. First hospital outbreak of the globally emerging *Candida auris* in a European hospital. Antimicrob. Resist. Infect. Control 5, 35 (2016). [PubMed: 27777756]
10. Supple L et al. Chlorhexidine only works if applied correctly: use of a simple colorimetric assay to provide monitoring and feedback on effectiveness of chlorhexidine application. Infect. Control Hosp. Epidemiol. 36, 1095–1097 (2015). [PubMed: 26074153]
11. Weiner LM, Webb AK, Walters MS, Dudeck MA & Kallen AJ Policies for controlling multidrug-resistant organisms in US healthcare facilities reporting to the National Healthcare Safety Network, 2014. Infect. Control Hosp. Epidemiol. 37, 1105–1108 (2016). [PubMed: 27350394]
12. Pacilli M et al. Regional emergence of *Candida auris* in Chicago and lessons learned from intensive follow-up at one ventilator-capable skilled nursing facility. Clin. Infect. Dis. 71, e718–e725 (2020). [PubMed: 32291441]
13. Adams E et al. *Candida auris* in healthcare facilities, New York, USA, 2013–2017. Emerg. Infect. Dis. 24, 1816–1824 (2018). [PubMed: 30226155]
14. Lockhart SR et al. Simultaneous emergence of multidrug-resistant *Candida auris* on 3 continents confirmed by whole-genome sequencing and epidemiological analyses. Clin. Infect. Dis. 64, 134–140 (2017). [PubMed: 27988485]
15. Larkin E et al. The emerging pathogen *Candida auris*: growth phenotype, virulence factors, activity of antifungals, and effect of SCY-078, a novel glucan synthesis inhibitor, on growth morphology and biofilm formation. Antimicrob. Agents Chemother. 61, e02396–16 (2017). [PubMed: 28223375]
16. Ostrowsky B et al. *Candida auris* isolates resistant to three classes of antifungal medications—New York, 2019. MMWR Morb. Mortal. Wkly Rep. 69, 6–9 (2020). [PubMed: 31917780]
17. Snitkin ES et al. Tracking a hospital outbreak of carbapenem-resistant *Klebsiella pneumoniae* with whole-genome sequencing. Sci. Transl. Med. 4, 148ra116 (2012).

18. Bishop L et al. Public Health England: Guidance for the Laboratory Investigation, Management and Infection Prevention and Control for Cases of *Candida auris* v2.0 https://www.gov.uk/government/publications/candida-auris-laboratory-investigation-management-and-infection-prevention-and-control (2017).
19. Chow NA et al. Tracing the evolutionary history and global expansion of *Candida auris* using population genomic analyses. mBio 11, e03364–19 (2020). [PubMed: 32345637]
20. Centers for Disease Control and Prevention, National Center for Emerging and Zoonotic Infectious Diseases. Screening for *Candida auris* Colonization https://www.cdc.gov/fungal/candida-auris/c-auris-screening.html (accessed 29 May 2020).
21. Tsay S, Kallen A, Jackson BR, Chiller TM & Vallabhaneni S Approach to the investigation and management of patients with *Candida auris*, an emerging multidrug-resistant yeast. Clin. Infect. Dis. 66, 306–311 (2018). [PubMed: 29020224]
22. Sherry L et al. Biofilm-forming capability of highly virulent, multidrug-resistant *Candida auris*. Emerg. Infect. Dis. 23, 328–331 (2017). [PubMed: 28098553]
23. Moore G, Schelenz S, Borman AM, Johnson EM & Brown CS Yeasticidal activity of chemical disinfectants and antiseptics against *Candida auris*. J. Hosp. Infect. 97, 371–375 (2017). [PubMed: 28865738]
24. Popovich KJ et al. Relationship between chlorhexidine gluconate skin concentration and microbial density on the skin of critically ill patients bathed daily with chlorhexidine gluconate. Infect. Control Hosp. Epidemiol. 33, 889–896 (2012). [PubMed: 22869262]
25. Findley K et al. Topographic diversity of fungal and bacterial communities in human skin. Nature 498, 367–370 (2013). [PubMed: 23698366]
26. Raz-Pasteur A, Ullmann Y & Berdicevsky I The pathogenesis of *Candida* infections in a human skin model: scanning electron microscope observations. ISRN Dermatol. 2011, 150642 (2011). [PubMed: 22363844]
27. Prohic A, Jovovic Sadikovic T, Krupalija-Fazlic M & Kuskunovic-Vlahovljak S *Malassezia* species in healthy skin and in dermatological conditions. Int. J. Dermatol. 55, 494–504 (2016). [PubMed: 26710919]
28. Zhu Y et al. Laboratory analysis of an outbreak of *Candida auris* in New York from 2016 to 2018: impact and lessons learned. J. Clin. Microbiol. 58, e01503–1 (2020). [PubMed: 31852764]
29. Nutman A et al. Detecting carbapenem-resistant Acinetobacter baumannii (CRAB) carriage: which body site should be cultured? Infect. Control Hosp. Epidemiol. 41, 965–967 (2020). [PubMed: 32618523]
30. Huang X et al. Murine model of colonization with fungal pathogen *Candida auris* to explore skin tropism, host risk factors and therapeutic strategies. Cell Host Microbe 29, 210–221 (2020). [PubMed: 33385336]
31. Rossow J. et al. . Factors associated with *Candida auris* colonization and transmission in skilled nursing facilities with ventilator units, New York, 2016–2018. Clin. Infect. Dis. 10.1093/cid/ciaa1462 (2020).
32. Snitkin ES et al. Integrated genomic and interfacility patient-transfer data reveal the transmission pathways of multidrug-resistant *Klebsiella pneumoniae* in a regional outbreak. Sci. Transl. Med. 9, eaan0093 (2017).
33. Prestel C et al. *Candida auris* outbreak in a COVID-19 specialty care unit—Florida, July–August 2020. MMWR Morb. Mortal. Wkly Rep. 70, 56–57 (2021). [PubMed: 33444298]

References

34. Thurlow CJ et al. Anatomic sites of patient colonization and environmental contamination with *Klebsiella pneumoniae* carbapenemase-producing *Enterobacteriaceae* at long-term acute care hospitals. Infect. Control Hosp. Epidemiol. 34, 56–61 (2013). [PubMed: 23221193]
35. Reichel M, Heisig P & Kampf G Pitfalls in efficacy testing—how important is the validation of neutralization of chlorhexidine digluconate? Ann. Clin. Microbiol. Antimicrob. 7, 20 (2008). [PubMed: 19046465]

36. Kampf G What is left to justify thÿe use of chlorhexidine in hand hygiene? J. Hosp. Infect. 70, 27–34 (2008).
37. Welsh RM et al. Survival, persistence, and isolation of the emerging multidrug-resistant pathogenic yeast *Candida auris* on a plastic health care surface. J. Clin. Microbiol. 55, 2996–3005 (2017). [PubMed: 28747370]
38. Edmiston CE Jr. et al. Preoperative shower revisited: can high topical antiseptic levels be achieved on the skin surface before surgical admission? J. Am. Coll. Surg. 207, 233–239 (2008). [PubMed: 18656052]
39. CLSI. Reference Method for Broth Dilution Antifungal Susceptibility Testing of Yeasts; Approved Standard—Third Edition (Clinical and Laboratory Standards Institute, 2008).
40. CLSI. CLSI document M27-A3 (Clinical and Laboratory Standards Institute, 2008).
41. Centers for Disease Control and Prevention, National Center for Emerging and Zoonotic Infectious Diseases (NCEZID), Division of Foodborne, Waterborne, and Environmental Diseases (DFWED). Antifungal Susceptibility Testing and Interpretation https://www.cdc.gov/fungal/candida-auris/c-auris-antifungal.html (2020).
42. Oh J et al. Biogeography and individuality shape function in the human skin metagenome. Nature 514, 59–64 (2014). [PubMed: 25279917]
43. Khot PD, Ko DL & Fredricks DN Sequencing and analysis of fungal rRNA operons for development of broad-range fungal PCR assays. Appl. Environ. Microbiol. 75, 1559–1565 (2009). [PubMed: 19139223]
44. Fadrosh DW et al. An improved dual-indexing approach for multiplexed 16S rRNA gene sequencing on the Illumina MiSeq platform. Microbiome 2, 6 (2014). [PubMed: 24558975]
45. Proctor DM et al. A spatial gradient of bacterial diversity in the human oral cavity shaped by salivary flow. Nat. Commun. 9, 681 (2018). [PubMed: 29445174]
46. DiGiulio DB et al. Temporal and spatial variation of the human microbiota during pregnancy. Proc. Natl Acad. Sci. USA 112, 11060–11065 (2015). [PubMed: 26283357]
47. Koren S et al. Canu: scalable and accurate long-read assembly via adaptive *k*-mer weighting and repeat separation. Genome Res. 27, 722–736 (2017). [PubMed: 28298431]
48. Vaser R, Sovic I, Nagarajan N & Sikic M Fast and accurate de novo genome assembly from long uncorrected reads. Genome Res. 27, 737–746 (2017). [PubMed: 28100585]
49. Langmead B & Salzberg SL Fast gapped-read alignment with Bowtie 2. Nat. Methods 9, 357–359 (2012). [PubMed: 22388286]
50. Walker BJ et al. Pilon: an integrated tool for comprehensive microbial variant detection and genome assembly improvement. PLoS ONE 9, e112963 (2014).

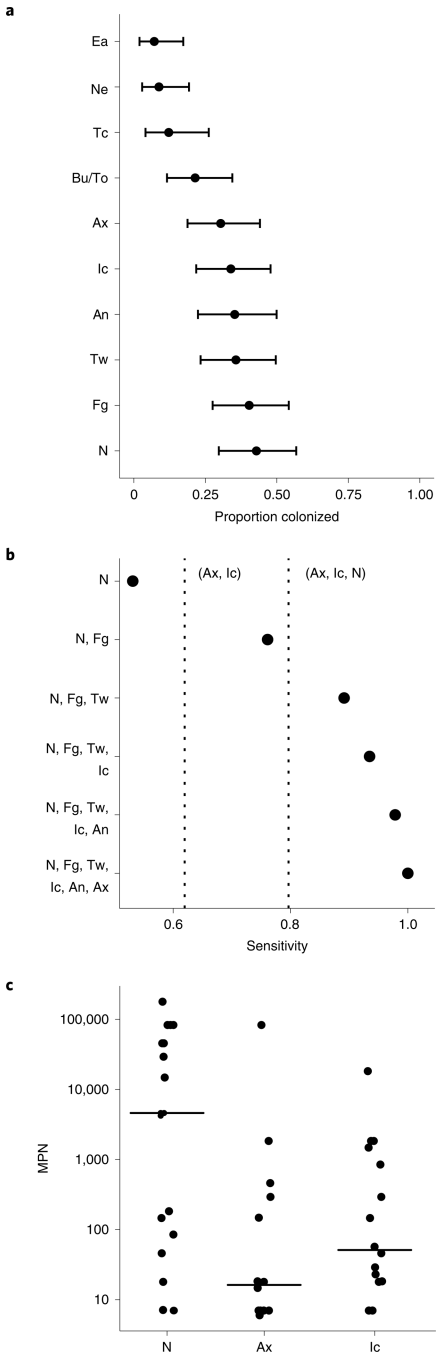

Fig. 1 |. Screening of multiple skin, nares, perianal and oral body sites for prevalence and individual-level bioburden of *C. auris* colonization.

a, The proportion of residents colonized at each body site. $n = 542$ independent samples of each of ten body sites of each of 57 residents at the time of the first screening. Data are presented as a point estimate ±95% confidence intervals. An, perianal skin; Ax, axilla; Bu, buccal mucosa; Ea, external auditory canal; Fg, palm and/or fingertips; Ic, inguinal crease; N, anterior nares; Ne, neck; Tc, tracheostomy; To, tongue; Tw, toe web. **b**, Sensitivity analysis to calculate the proportion of colonized residents captured by screening different

groupings of sites. Sensitivity is defined as the proportion colonized at each site grouping divided by the total number of residents identified as colonized at any body site. Dashed vertical lines correspond to the sensitivity of two routine screening strategies targeting the body sites axilla and inguinal crease (left dashed line) and axilla, inguinal crease and nares (right dashed line). A minimum of six sites was required to achieve 100% sensitivity, capturing all colonized individuals. **c**, Number of viable *C. auris*, determined by the MPN, plotted for the inguinal crease ($n = 16$), nares ($n = 19$) and axilla ($n = 16$). Groupwise medians are demarcated with black lines. Statistical significance of differences between sites was assessed with the Kruskal–Wallis test ($P < 0.05$).

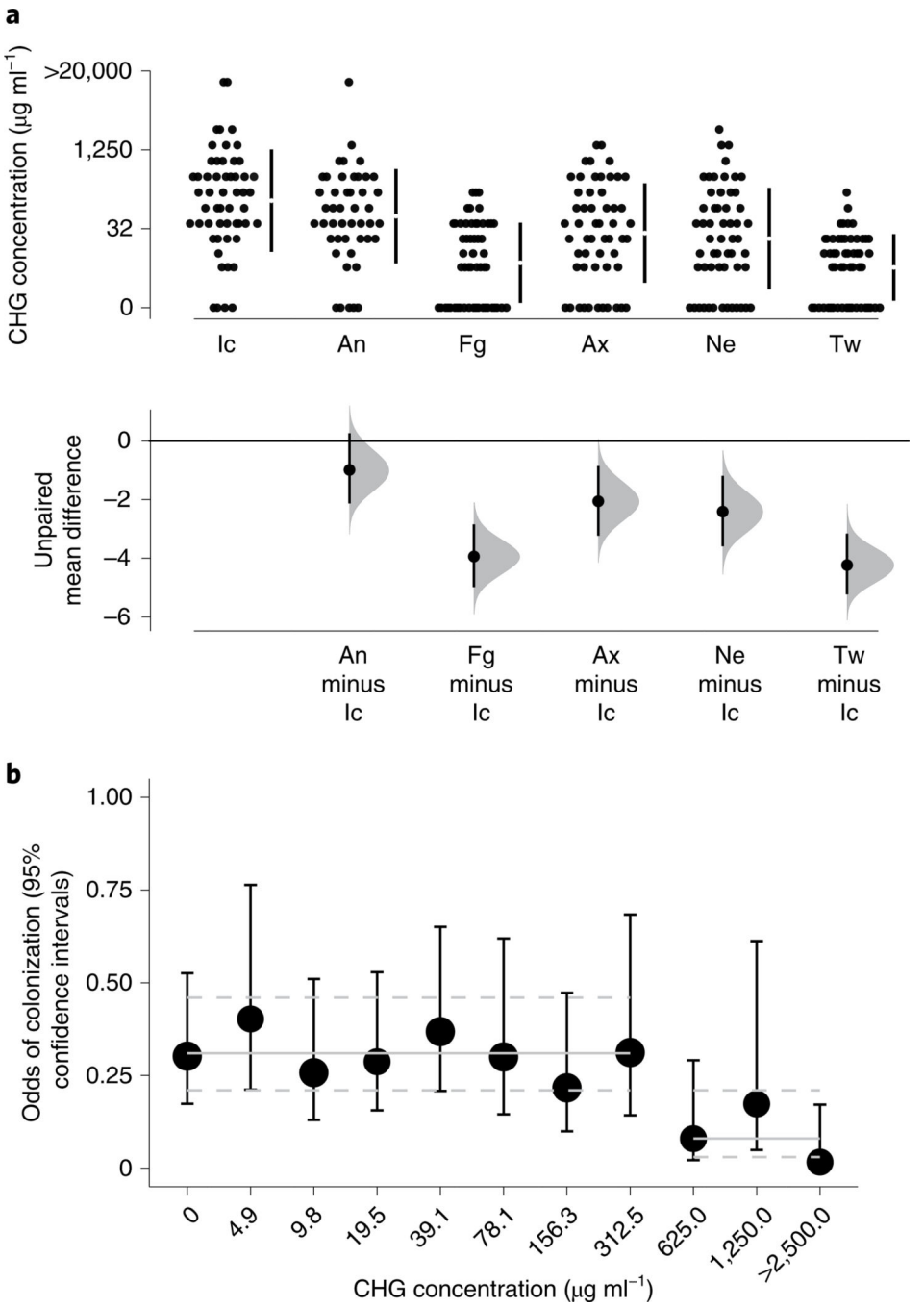

Fig. 2 |. High concentrations of CHG are needed to reduce the odds of *C. auris* colonization.
a, Gardner–Altman estimation plot comparing the mean difference in CHG concentrations (μg ml^{-1}) across body sites. Top, raw data are shown as a scatterplot of CHG concentration plotted as a function of body site for the first survey (54 residents, n = 319). Bottom, data are presented as the mean difference between CHG concentration (μg ml^{-1}) at each body site and the inguinal crease, the site reaching the highest average CHG concentration, ±95% confidence intervals. Histograms reflect the sampling distribution from a nonparametric bootstrap. **b**, Each point represents the modeled odds of *C. auris* colonization (±95%

confidence intervals) plotted against the measured skin CHG concentration (μg ml^{-1}), adjusted for multiple measurements within resident and over time. The solid horizontal lines represent odds of colonization per respective group (that is, <625 μg ml^{-1} versus ≥625 μg ml^{-1}), while the dashed lines encompass the 95% confidence interval surrounding each group estimate. Significance tests were based on the model-estimated log odds divided by the standard error, distributed as *a t* distribution.

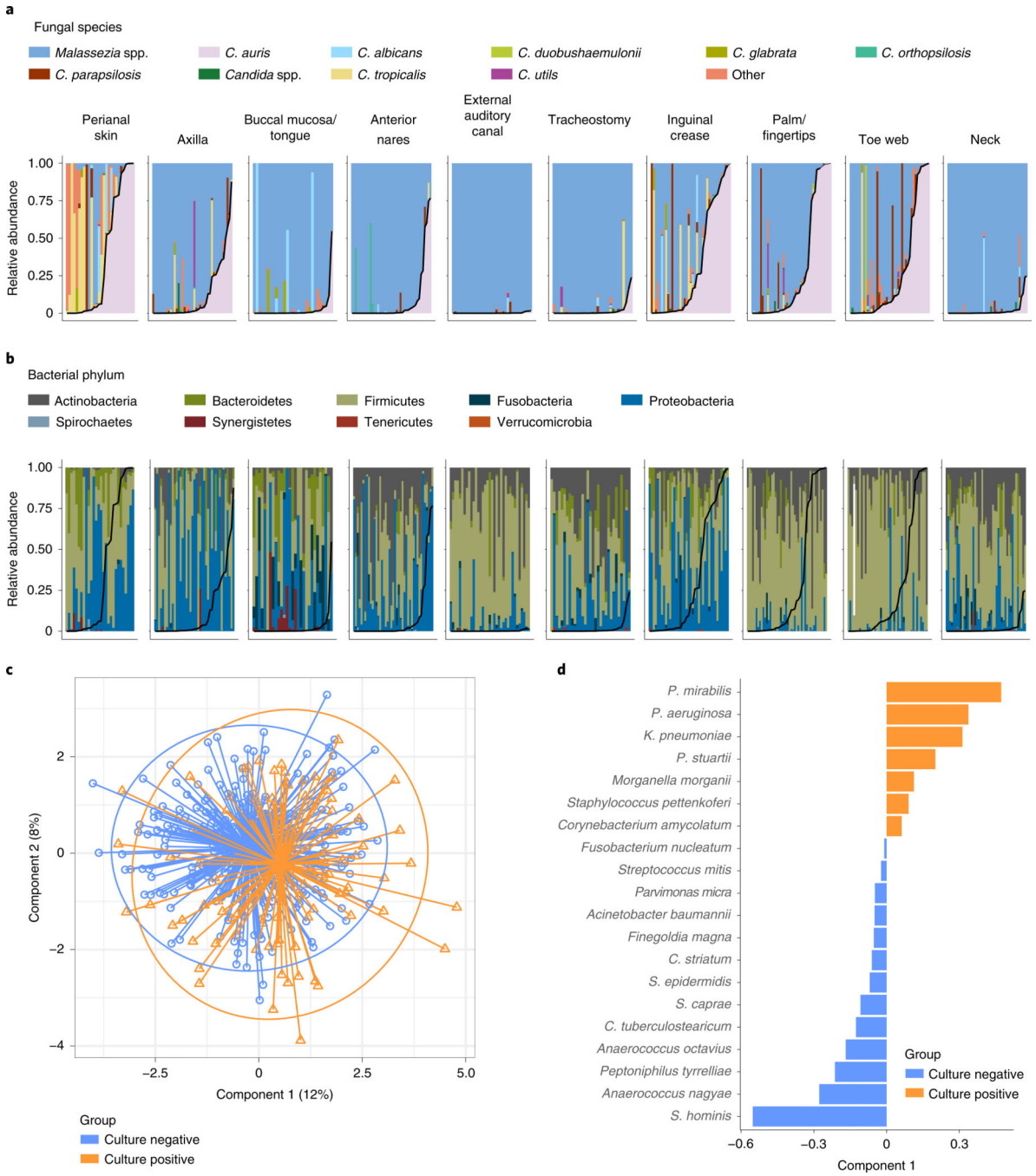

Fig. 3 |. Underlying skin microbiome (fungal and bacterial communities) integrated with *C. auris*–colonization status.

Panels represent the body-site-specific relative abundance of fungal (**a**) or bacterial (**b**) organisms. Bars represent the 51 participants, ordered by *C. auris* abundance. The inner black curve represents the relative abundance of *C. auris* for each sample for each participant. **a**, Relative abundance of fungal species at each body site surveyed for each participant. Colors correspond to fungal genera or individual *Candida* spp. Genera included in the 'other' category include *Saccharomyces*, *Trichosporon*, *Trichophyton* and *Aspergillus*.

b, Relative abundance of bacteria, colored by phylum, reveals site-specific associations of *C. auris* with Proteobacteria. **c**,**d**, Colors correspond to sample or loadings associated with culture negativity or positivity. **c**, Sample projection across first and second components of sPLS-DA. **d**, Variable loadings across the first sPLS-DA component.

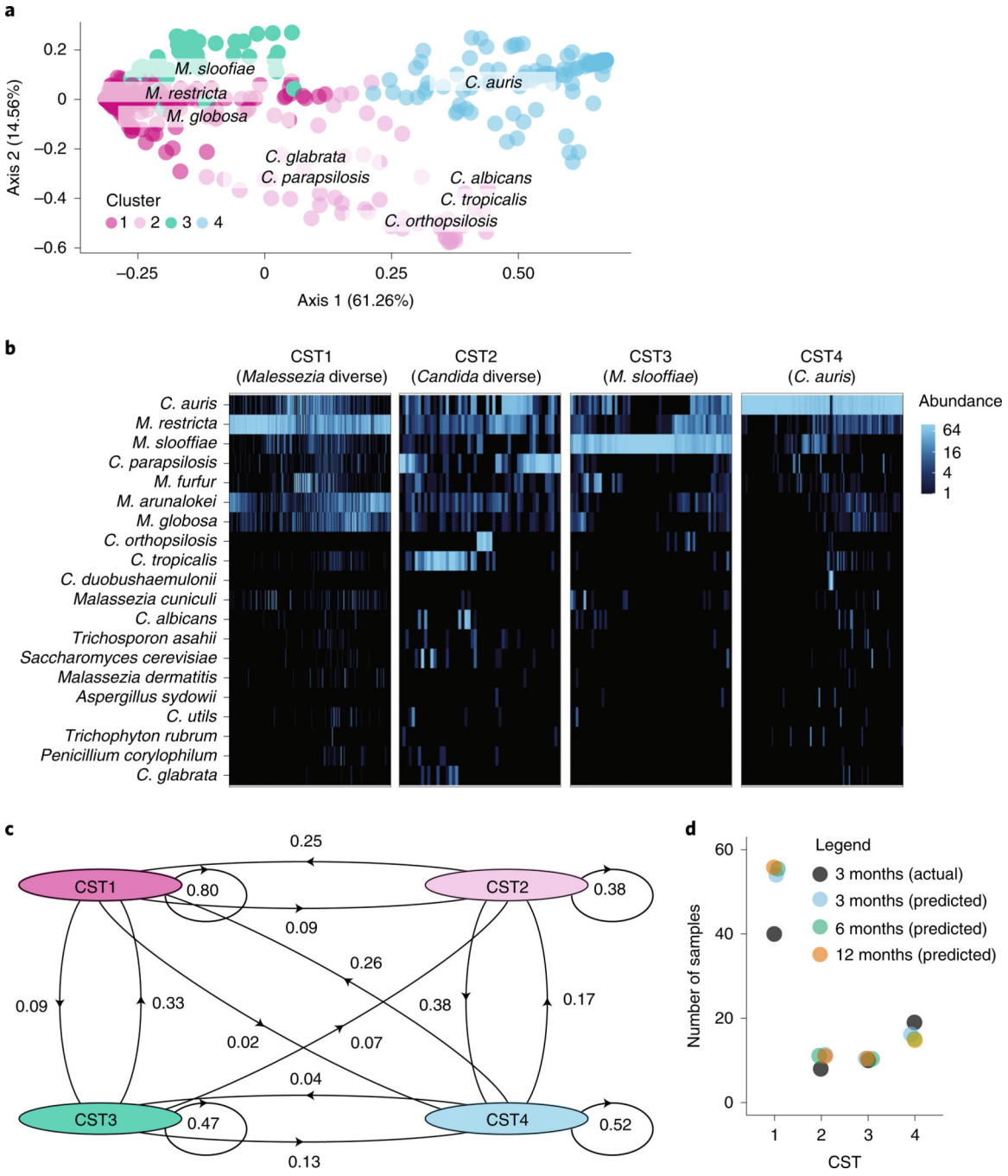

Fig. 4 |. Skin fungal communities, dominated by *Malassezia* and *Candida* species, have differential stability, resilience and likelihood of invasion by *C. auris*.

a, Principal-coordinate analysis of the weighted UniFrac metric of the fungal community at each body site (toe webs, fingertips and/or palm, inguinal crease, anterior nares). Samples are shaded according to CST identity, as revealed by 'partition around medoids' analysis. CST1 tends to be dominated by *M. restricta* (N = 256, 53.0%), CST2 by a variety of *Candida* species (N = 52, 10.7%), CST3 by *M. slooffiae* (N = 62, 12.8%) and CST4 by *C. auris* (N = 113, 23.4%). Segregation of *Malassezia* and *Candida* species across the first axis

explains 61% of the variance. *Candida* species segregate across the second major axis, which accounts for ~15% of the variance. **b**, Relative abundance of the top 20 species in each sample, clustered by CST. Shading is based on the relative abundance of taxa within each sample. **c**, Self and interstate transition probabilities inferred for samples of the toe webs, palm and/or fingertips, inguinal crease and anterior nares. **d**, Scatterplot of the predicted numbers of samples in each CST at 3, 6 and 12 months after sample collection compared to the actual number of samples at 3 months. Predictions were generated using the Markov chain in **c**.

Table 1 |

Bivariate associations of clinical characteristics with *C. auris*-colonization status at the time of the first survey

	Colonized (*n* = 46)	**Not colonized (*n* = 11)**	**OR (95% CI)**	***P* value**
Length of stay (d) between admission and first swab (M ± IQR)	361 ± 801	571 ± 1,372	1.00 (0.99,1.00)	0.26
Age in years (mean ± s.d.)	59 ± 14	59 ± 14	1.00 (0.95,1.05)	0.89
Female (*n* (%))	18 (39)	5 (45)	0.77 (0.20,2.91)	0.74
African American (*n* (%))	31 (74)	9 (90)	0.31 (0.066,2.76)	0.42
Mechanical ventilation (*n* (%))	23 (50)	0 (0)	23.00 (1.28,413.3)	0.002
Gastrostomy tube (*n* (%))	35(78)	3 (27)	9.33 (2.08,41.89)	0.003
Tracheostomy (*n* (%))	34 (74)	6 (55)	2.36 (0.61,9.17)	0.27
Urinary catheter (*n* (%))	33 (72)	3 (27)	6.77 (1.55,29.56)	0.012
Hospital stay within past 90d (*n* (%))	20 (44)	3 (27)	2.13 (0.50,9.11)	0.5
Charlson comorbidity index (M ± IQR)	3 ± 2	3 ± 2	0.91 (0.65,1.28)	0.59
Congestive heart failure (*n* (%))	10 (22)	5 (45)	0.33 (0.084,1.32)	0.11
Chronic lung disease (*n* (%))	36(78)	6 (55)	3.00 (0.76,11.90)	0.11
Braden scale score[a] (mean ± s.d.)	13 ± 2	16 ± 5	0.74 (0.59,0.94)	0.013
History of carbapenemase- producing bacterial colonization or infection[b]	31 (67)	6 (55)	1.72 (0.45,6.56)	0.49
Antibacterial receipt in prior 90 d (*n* (%))	34 (74)	5 (45)	3.4 (0.88,13.21)	0.030
Antifungal receipt in prior 90 d (*n* (%))	5 (11)	0 (0)	3.05 (0.16,59.29)	0.57

[a]The Braden Scale for Predicting Pressure Sore Risk assesses a person's risk of developing a pressure ulcer by examining six criteria: moisture, activity, mobility, nutrition and friction and shear.

[b]Screening of facility residents for carbapenemase-producing bacterial colonization was performed routinely. Screening for colonization by other multidrug-resistant organisms was not performed.

CI, confidence interval; IQR, interquartile range; M, median; OR, odds ratio.